AN INVESTIGATION ON PRODUCTION OF SEMIKILLED STEEL WITH MARGINAL POROSITY

By

DIPAK MAZUMDAR
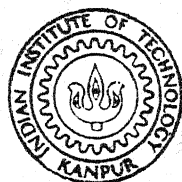
DEPARTMENT OF METALLURGICAL ENGINEERING

INDIAN INSTITUTE OF TECHNOLOGY KANPUR

AN INVESTIGATION ON PRODUCTION OF SEMIKILLED STEEL WITH MARGINAL POROSITY

A Thesis Submitted
in Partial Fulfilment of the Requirements
for the Degree of

MASTER OF TECHNOLOGY

By

DIPAK MAZUMDAR

to the

DEPARTMENT OF METALLURGICAL ENGINEERING

INDIAN INSTITUTE OF TECHNOLOGY KANPUR

DEDICATED TO SRI ASHISH SENGUPTA

MY TEACHER AT S.P.H.S. SCHOOL,

DHUBRI

ASSAM

C E R T I F I C A T E

Certified that this work on ''An Investigation on Production of Semikilled Steel with Marginal Porosity'' has been carried out by Dipak Mazumdar under my supervision and that it has not been submitted elsewhere for a degree.

A. Ghosh
Professor
Department of Metallurgical Eng
Indian Institute of Technolog
Kanpur- 208016

ACKNOWLEDGEMENT

It is a pleasure to express a deep sense of gratitude and appreciation to Professor A. Ghosh for his able guidence and encouragement during the course of this investigation.

I am extremely grateful to Mr.D.V. Singh, Deputy Manager (SMS), Field Gun Factory, Kanpur for the help rendered by him during the course of this investigation. I have also been helped more than I can say in preparing this thesis by the kind help of colleagues Mr.D. Ghosh, Mr.Sanat Choudhury, Mr.D.R. Kulkarni and Miss. B. Rama Devi for initial trials of experimental work.

My thanks are also due to Mr.A. Sharma, Mr.S.R. Chaurasia, Mr.Sukdev Singh, Mr.B.Sachan for their assistance specially during the steelmelting experiments. I am particularly grateful to Mr.B.D. Biswas for typing the manuscript and providing me company throughout my stay at IIT/K.

Financial assistance by DST during the initial period of the study is gratefully acknowledged.

I cannot hope that this piece of work is now entirely free of errors and obscurities, but I am certain that it is a good deal clearer and more accurate than it could have been without all the generous assistance I have been fortunate enough to receive.

I.I.T. Kanpur

November, 1982

DIPAK MAZUMDAR

CONTENTS

LIST OF FIGURES

LIST OF TABLES

P_b — pressure inside a bubble, dynes cm^{-2}.

P_o — atmospheric pressure, dynes cm^{-2}.

P_l — pressure due to static head of liquid, dynes cm^{-2}.

r^φ — radius of the critical nucleus, cm.

P_{ex}^φ — excess pressure inside the bubble at critical nucleus size, dynes cm^{-2}.

σ — surface tension of molten metal, dynes cm^{-1}.

P_T — total thermodynamic pressure of gases ($= p_{CO} + p_{H_2} + p_{N_2}$ i.e., the sum of seperate partial pressures of CO, H_2 and N_2 respectively in equilibrium with molten steel), atm.

C_o — the initial uniform solute content of the liquid, mole cm^{-3} or g cm^{-3}.

C_s — concentration of the solute in solid, mole cm^{-3} or g cm^{-3}.

C_l — concentration of the solute in liquid, mole cm^{-3} or g cm^{-3}.

K — equilibrium distribution/partition coefficient

g — fraction of original volume of interdendritic liquid solidified.

C_O', C_O'' — concentration of oxygen in the liquid phase at succeeding stages of solidification g' and g'' respectively, moles cm^{-3} or g cm^{-3}.

C_{Si}', C_{Si}'' — concentration of silicon in the liquid phase at succeeding stages of solidification g' and g'' respectively, moles cm^{-3} or g cm^{-3}.

C_{Mn}', C_{Mn}'' — concentration of manganese in the liquid phase at succeeding stages of solidification g' and g'' respectively, moles cm^{-3} or g cm^{-3}.

c_0 equilibrium concentration of oxygen in the liquid phase after deoxidation reaction at solidification g'', moles cm^{-3} or $g\ cm^{-3}$.

c_{Si} equilibrium concentration of manganese in the liquid phase after deoxidation reaction at solidification g'', moles cm^{-3} or $g\ cm^{-3}$.

c_{Mn} equilibrium concentration of manganese in the liquid phase after deoxidation reaction at solidification g'', moles cm^{-3} or $g\ cm^{-3}$.

γ composition of silicate formed as a result of deoxidation reaction at solidification g''.

K_{12} equilibrium constant defined by equation (1.12)

K_{13} equilibrium constant defined by equation (1.13)

K_{16} equilibrium constant defined by equation (1.16)

K_{17} equilibrium constant defined by equations (1.17) and (1.18).

K_{19} equilibrium constant defined by equation (1.19)

K_{20} equilibrium constant defined by equation (1.20)

K_3 equilibrium constant defined by equation (3.3)

K_6 equilibrium constant defined by equation (3.6)

K_{11} equilibrium constant defined by equation (3.11)

h_0, h_C, h_N, h_H henrian activity of oxygen, carbon, nitrogen and hydrogen respectively.

p_{CO} partial pressure of carbon monoxide in the volume of interdendritic liquid, atm.

p_{H_2} partial pressure of hydrogen in the volume of interdendritic liquid, atm.

p_{N_2} partial pressure of nitrogen in the volume of interdendritic liquid, atm.

A B S T R A C T

Melting and casting of steel was carried out in the laboratory under controlled atmosphere. The programme included controlled deoxidation, chemical analysis of elements includin; total oxygen content, dissolved oxygen content and nitrogen. I· was found that the total oxygen contents of steel were signifi- cantly larger than the values of dissolved oxygen content.

Sliced ingots were classified as dense, marginally porous and porous. Attempts were made to correlate this with the predictions based on thermodynamic model of Harkness, Nicholson and Murray[11]. Such comparisons showed that ingots tended to exhibit more porosity as compared to theoretical predictions. This has been attributed to pick up of oxygen from the atmosphere during teeming.

Experimentally measured values of dissolved oxygen in molten steel scattered around the values of the same as calculated thermodynamically for deoxidation by silicon and manganese.

CHAPTER I

INTRODUCTION

I.1. OBJECTIVE[1,2,3]

The intensity of gas evolution during ingot casting is determined by the degree of deoxidation of the steel at the time it enters the mould, by its fluidity, the rate of solidification, the teeming temperature and by its chemical composition including hydrogen and nitrogen content. From the point of view of gas formation, the cast ingots may be classified as :

(i) Killed steel, which exhibits neither gas formation nor blowhole formation,

(ii) Semi-killed steel, where there is some gas formation as well some blowhole formation, but negligible gas evolution,

and (iii) Rimming steel, which exhibits vigorous gas formation and gas evolution followed by blowhole formation.

Killed steel ingots are well deoxidised and are characterised by the formation of a shrinkage cavity in the top portion of the castings, which in practice used to be cut off prior to any mechanical processing of the cast ingot. This accounts for a considerable loss of ingot yield. However methods have been developed that make it possible to eliminate the shrinkage cavity. These include :

(i)   Supply of molten metal from the feeder head to make up the contraction during solidification,

(ii)   a hot top practice,

and (iii) addition of antipiping compounds like calcium etc. in the mould during the latter stage of solidification.

Nevertheless there are certain inherent demerits associated with these practices, such as :

(i)   an additional mechanical assembly is required in (i) and (ii), which increases the complexiety of operation,

(ii)   the addition of antipiping compounds makes the resultant ingot rich in inclusion content and thus introduces certain limitations to the use of the cast ingot,

and (iii) less yield.

Because of these short comings associated with the production of killed steel ingots, the world trend is to produce more semikilled and rimming steel ingots than killed steel ingots. Production of rimming steel ingots is associated with a number of advantages over that of the killed steel ingots. These include :

(i)   less consumption of deoxidisers, which inturn offers better economy,

(ii)   more yield,

and (iii) good mechanical properties, ensured by the presence of a dense skin.

In our country, however, the trend is to produce more semi-killed steel than rimming steel. This is primarily because of inadequate operating controls in almost all our plants. One of the prime controlling factors, which ensures a good rimming steel ingot is the temperature of the molten metal at the time it enters the mould. Practice shows that a temperature in the viccinity of $1560^{\circ}C$ to $1570^{\circ}C$ is considered essential for the production of a quality rimming steel ingot. Owing to poor process control, the desirable temperature is not achieved during most of the rimming castings and with the result inferior quality ingots result.

Semikilled steel however can be produced more easily than rimming steel. Depending upon the extent of deoxidation a series of semi-killed steel may result. Fig(I-1) shows an ideal semi-killed structure, in which as a result of controlled deoxidation, blowholes form only at the top of ingot and counterbalance the shrinkage, to produce almost a flat top ingot. This type of ingot structure can be obtained by incomplete deoxidation in the ladle, and subsequent correction by adding deoxidisers in the mould, or by mechanical or chemical capping. In our country, however, water quenching of the ingot top is normally practised to achieve such a structure. This practice, which ensures a flat top maynot satisfy the other necessary requirements (i.e. dense ingot, blowholes only at the top etc.), unless deoxidation is carried out to the optimum level. In advanced countries,
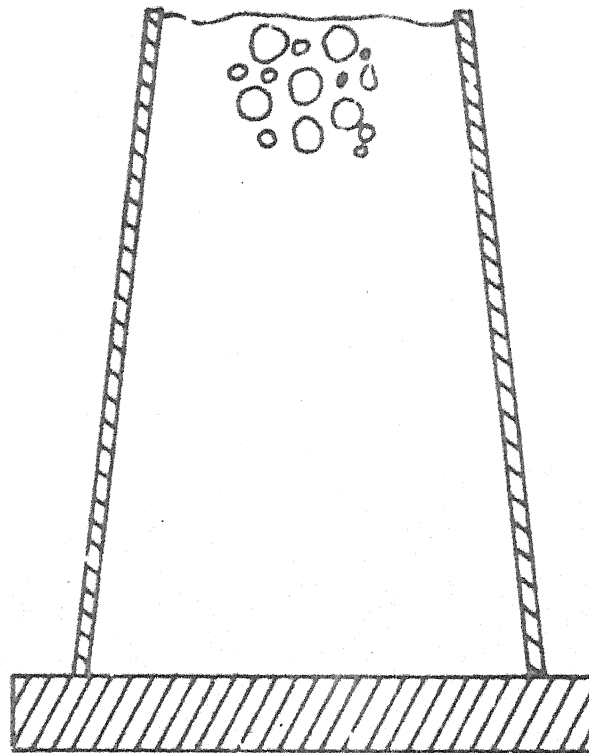
FIG. I.1 TYPICAL MACROSTRUCTURE
OF AN IDEAL SEMIKILLED
STEEL INGOT

combined deoxidation in ladle and mould is sometimes pra-
ctised to obtain an ideal semi-killed structure, though
deoxidation in the ladle is the most common, and the ing-
ots thus produced are referred to as the ladle-balanced
ingots. Towards obtaining such a structure, the desirable
teeming practice should be ladle balancing (i.e., addition
of deoxidisers in ladle only). However the current teeming
practice in vogue in India employ very little or practica-
lly no ladle balancing but considerable mould deoxidation.
This trend in ingot casting may account for a considerable
deviation from the desired ingot morphology, owing to a
number of limitations associated with it.

The reasons attributed above make the features
of blowhole formation in semi-killed steel a worthy field of
investigation. Accordingly, the objective of the present stu-
dy was to conduct laboratory investigation in this particular
direction along with physico-chemical interpretation of the
entire process. This work was essentially aimed to test the
emperical findings of Harkness et al[11] which will be outlined
elaborately in the succeeding sections.

I.2   LITERATURE REVIEW

I.2.1   Physical chemistry of blowhole formation during
solidification of semi-killed steel ingots

Blowholes form in rimming steel as well as in
various grades of semi-killed steel. However when the mould
is not properly cleaned, blowholes may even form in a killed
steel ingot, particularly in the region close to the mould-
wall. Considering this particular case of blowhole formation
in killed steel ingots as insignificant, it will not be dis-
cussed here.

A rimming steel ingot is hardly deoxidised and
contains appreciable amount of dissolved gases, particularly
oxygen (0.03 - 0.06 wt pct.). Such an ingot is characterised
by violent evolution of carbon monoxide during the progress
of solidification mentioned in the preceeding section. Bulk
of the carbon monoxide evolved escapes to the free surface,
since the top portion of the ingot remains molten for a long
time owing to the circulation current. A part of it is only
entrapped. Nucleation, growth and entrapment of gas bubble
in rimming steel has been discussed elaborately elsewhere[4]
and hence is not reproduced here,

Depending upon the extent of deoxidation, there
may be a series of semi - killed grades of steels. The mech-
anism of blowhole formation in semi - killed steel exhibits
marked difference depending on how such an ingot structure is
approached from either the killed side or the rimming side.
As a part of the present study, we shall restrict ourselves
to the mechanism of blowhole formation in semi-killed steels
when such a structure is approached from the killed end.

Approaching from the killed steel side, the formation of blowholes in castings is expected to exhibit three distinct stages, viz. nucleation, growth and entrapment. That is to say that if a gas bubble can nucleate and it grows to some size, and if that bubble is entrapped, blowhole will result. Hence the conditions should be such that nucleation is possible, and is given by

$$r^{\varphi} = \frac{2\sigma}{P_{ex}^{\varphi}} \qquad \dots\dots \quad (1.1)$$

where,

r^{φ} = radius of critical nucleus, Cm

σ = the surface tension of the molten metal, dynes/Cm,

and P_{ex}^{φ} = excess pressure inside the bubble at critical nucleus size, dynes/Cm^2,

P_{ex}^{φ} is defined by :

$$P_b = P_o + P_1 + P_{ex}^{\varphi} \qquad \dots\dots \quad (1.2)$$

where,

P_b = Pressure inside a bubble,

P_o = Atmospheric pressure

and P_1 = Pressure due to static head of liquid

Experimental results with molten steel[5,6] and with cold models[4,7] show that P_{ex}^{φ} is less than 1 atm. in most cases. This has been explained as due to entrapped gas (or air) already present in tiny pores etc. eliminating the need for nucleation so that bubbles can grow easily. Therefor

it is customary to assume P_{ex}^{φ} to be zero, and hence the thermodynamic criterion for blowhole formation becomes

$$P_b = P_o + P_l \qquad \text{.......} \quad (I.3)$$

There are two possible modes of nucleation viz. homogeneous nucleation and heterogeneous nucleation. Homogeneous nucleation of gas bubble requires supersaturation of the liquid to such an extent is not possible owing to the limit of solubility. However gas bubble formation is considered most likely to occur at a solid/liquid interface during solidification, since it is here the solute elements are rejected from the solidifying metal. The nucleation of the bubble at the solid/liquid interface establishes the fact that the phenomenon of nucleation is essentially heterogeneous in nature.

From physico - chemical point of view, a bubble grows if

$$P_T \quad \rangle \quad P_b$$

where,

P_T = total thermodynamic pressure of gases (= $p_{CO} + p_{H_2} + p_{N_2}$ i.e. the sum of seperate partial pressures of CO, H_2 and N_2 respectively in equilibrium with molten steel).

As pointed out earlier, bubbles primarily form at solid/liquid interface during ingot casting. If the interface is flat and vertical, a very tiny bubble may remain attached to it due to surface tension forces but it gets detached when it is significant in size. On the other hand bubbles inside interdendritic space may remain entrapped and form blowholes such as

tubular primary blowholes. If the top gets forzen early then also gases would form blowholes. Higher is $(P_T-P_o-P_1)$ more is the chance of bubble escape and consequently less blowhole formation. Intensity and pattern of fluid flow is important as it can cause bubble escape by drag as well as impact.

By using appropriate physio-chemical model for enrichment of solutes and thermodynamic data for deoxidation reactions in steel, it is possible to calculate the partial pressure of gases (p_{CO}, p_{H_2}, and p_{N_2}) and total pressure P_T at each stage of solidification.

A detailed physio-chemical analysis of reactions taking place during solidification of steel was first made by Turkdogan[8] and is outlined below :

As the liquid becomes richer in impurities during dendritic solidification of steel, a series of reaction may occur in the liquid phase trapped within the branches of growing dendrite platelets. Because of the strong interaction between dissolved oxygen and impurites in liquid steel, the reactions most likely to occur are of the deoxidation type. Impurity enrichment in the interdendritic liquid with the progress of solidification is a complex process and an accurate mathematical formulation of the problem is possible only for known boundary conditions during freezing.

Since the diffusivity of carbon, hydrogen and nitrogen are large in liquid steel phase at high temperature, it was assumed that these elements were completely mixed in the solid and liquid phases during solidification. This meant that

at any stage of solidification there was no concentration gradient of these elements and the partition occurs accor,ing to the equilibrium distribution coefficient k, where $k = \frac{C_s}{C_1}$, where C_s and C_1 are concentrations of the solute in solid and liquid respectively at equilibrium with one another. Assuming linearity of both solidus and liquidus curves, the concentration of carbon, hydrogen and nitrogent were calculated from the following expression :

$$\frac{C_1 - C_o}{C_o - C_s} = \frac{g}{(1-g)} \quad \ldots\ldots\ldots \quad (1.4)$$

or,

$$C_1 = \frac{C_o}{[1-(1-k)g]} \quad \ldots\ldots\ldots \quad (1.5)$$

where,

C_o = the initial uniform solute content of the liquid,

g = the fraction of original volume of interdendritic liquid solidified,

and k = the equilibrium distribution coefficient. The appropriate equation for each element was derived by substituting the characteristic k value in the foregone equation.

The interdiffusivities of manganese and silicon in liquid iron at $1500^{\circ}C$ to $1600^{\circ}C$ are in the range of 10^{-5} to $10^{-4} \, Cm^2 Sec^{-1}$. In the solid iron near the melting temperature these diffusivities are lowered by about two orders of magnitude. On the basis of this information it was assumed that there would be complete mixing in the liquid phase, but mixing in the solid would be negligible. Scheil[9] and later Pfann[10] derived equation for a binary system, which was adopted by Turkdogan. According to it,

$$\frac{C_s}{k} = C_1 = C_o (1-g)^{k-1} \quad \ldots\ldots\ldots \quad (1.6)$$

In the present calculation, constant distribution coefficient was taken for silicon and manganese. Therefore for these two solutes, enrichment in the liquid was computed using the following expression as derived from equation (1.6) for k = 2/3

$$C_1 = \frac{C_o}{(1-g)^{1/3}}$$ .... (1.7)

The estimation of oxygen enrichment in solidifying liquid steel is less certain. For the present purpose the following equation was used :

$$C_1 = \frac{C_o}{1-g}$$ .... (1.8)

which is theoretically correct only for the limiting case of k ⟶ 0 .

Fig. (I-2) shows the extent of solute enrichment (no interaction between them) in freezing liquid steel initially containing 0.5 pct. Mn, 0.05 pct. C, 0.02 pct. Si, and 0.01 pct O.

In calculating the oxygen enrichment in the entrapped freezing liquid, due account was taken of the deoxidation reaction, which is expected to play a paramount role in controlling the oxygen content of the liquid. The author in his approach had considered a deoxidation reaction analogous to the complex deoxidation by silico-manganese.

If at a particular stage of solidification g' , the remaining liquid phase containing C_o' pct. O, C_{Si}' pct. Si and C_{Mn}' pct. Mn in equilibrium with the deoxidation product manganese-silicate then on further solidification at g'',
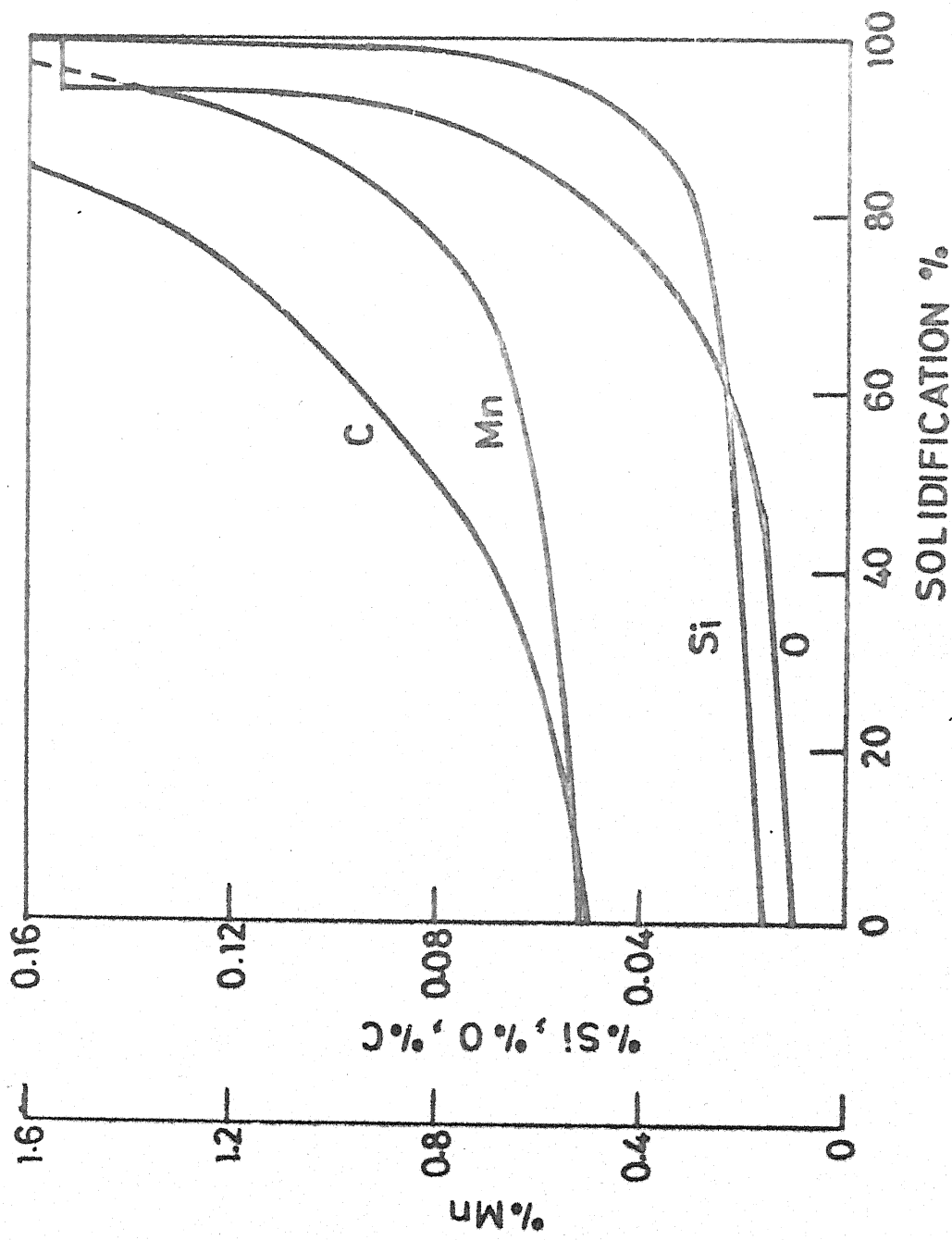
FIG. 1.2 SOLUTE ENRICHMENT IN SOLIDIFYING LIQUID
STEEL IF NO REACTION TAKES PLACE BETWEEN
THE SOLUTES OF IRON

concentrations of solutes as calculated by equation (I.8)
and (I.7) would be C'_0 pct. 0, C''_{Si} pct. Si and C''_{Mn} pct.
Mn. Since these new concentrations are above those for
Si/Mn - O deoxidation reactions, they react forming more
manganese-silicate. The mass balance on the amount of
solutes consumed was given by the equation

$$\triangle C_0 = \frac{32}{28.09} \triangle C_{Si} + \frac{16}{54.94} \triangle C_{Mn} \quad \ldots\ldots\ldots \quad (I.9)$$

where $\triangle$ signified the amounts used. Thus,

$$\triangle C_0 = C''_0 - C_0$$

$$\triangle C_{Mn} = C''_{Mn} - C_{Mn}$$

and $\quad \triangle C'_{Si} = C''_{Si} - C_{Si}$

where the second concentration term without prime represent
equilibrium concentrations of solutes after deoxidation re-
action at solidification g''. Representing the composition
of silicate formed by the parameter $\gamma (= \frac{N_{MnO}}{N_{SiO_2}})$, the stoichi-
ometric requirements yielded

$$\triangle C_{Mn} = \frac{54.94}{28.09} \gamma \triangle C_{Si} \quad \ldots\ldots\ldots \quad (I.10)$$

By combining equations (I.9) and (I.10) the following expre-
ssion was obtained

$$C''_0 - C_0 = 0.57(2+\gamma)(C''_{Si} - C_{Si}) \quad \ldots\ldots \quad (I.11)$$

Furthermore, since the concentration C_0, C_{Si} and C_{Mn} were
assumed to be in equilibrium with a particular deoxidation
product $\gamma = \frac{N_{MnO}}{N_{SiO_2}}$, the following equilibria were considered

$$[Mn]+[O] = MnO(s) \; ; \; K_{12} = \frac{N_{MnO}}{[\% \, Mn][\% \, O]} \quad \ldots \quad (I.12)$$

and

$$[Si]+2(MnO)(s) = 2[Mn]+(SiO_2)(s) \; ; \; K_{13} = \frac{[\% \, Mn]^2 (a_{SiO_2})}{[\% \, Si](a_{MnO})^2}$$

$$(I.13)$$

Incorporation of these two equations, together with equations (1.7) and (1.8) for manganese, silicon and oxygen in equation (1.11) gave the final expression, viz.

$$C_0' \frac{1-g'}{1-g''} - \frac{a_{MnO}}{K_{12}C_{Mn}} = 0.57 \left[2+ \frac{N_{MnO}}{N_{SiO_2}}\right] \left[C_{Si}'\left(\frac{1-g'}{1-g''}\right)^{1/3} - \frac{[C_{Mn}]^2 (a_{SiO_2})}{K_{13}(a_{MnO})^2}\right] \qquad \ldots\ldots\ldots \quad (1.14)$$

For given values of C_0', C_{Si}' and C_{Mn}' at fractional solidification g' and for the known values of equilibrium constants, K_{12} and K_{13}, at the freezing temperature, equation (1.14) was solved by a trial and error method for various values of a_{MnO}, a_{SiO_2}, and N_{MnO}/N_{SiO_2}. After computing the composition of manganese silicate, thus formed at solidification g'', equilibrium solute concentrations were readily calculated in the usual manner. In the above calculations the supersaturation of the reactants required for the occurence of the reaction was assumed to be negligibly small.

Fig. (I-3) illustrates the change in the oxygen content of the entrapped liquid during freezing of steel. The figure shows that as the level of initial silicon content in the metal is increased, deoxidation reaction commences at an early stage of solidification. However the curves in the figure approach the manganese deoxidation curve towards the latter stage of solidification.

Besides manganese silicate, solid silica also form as deoxidation product when a critical [% Si]/[% Mn] ratio is reached. For such a case only silicon should be considered in
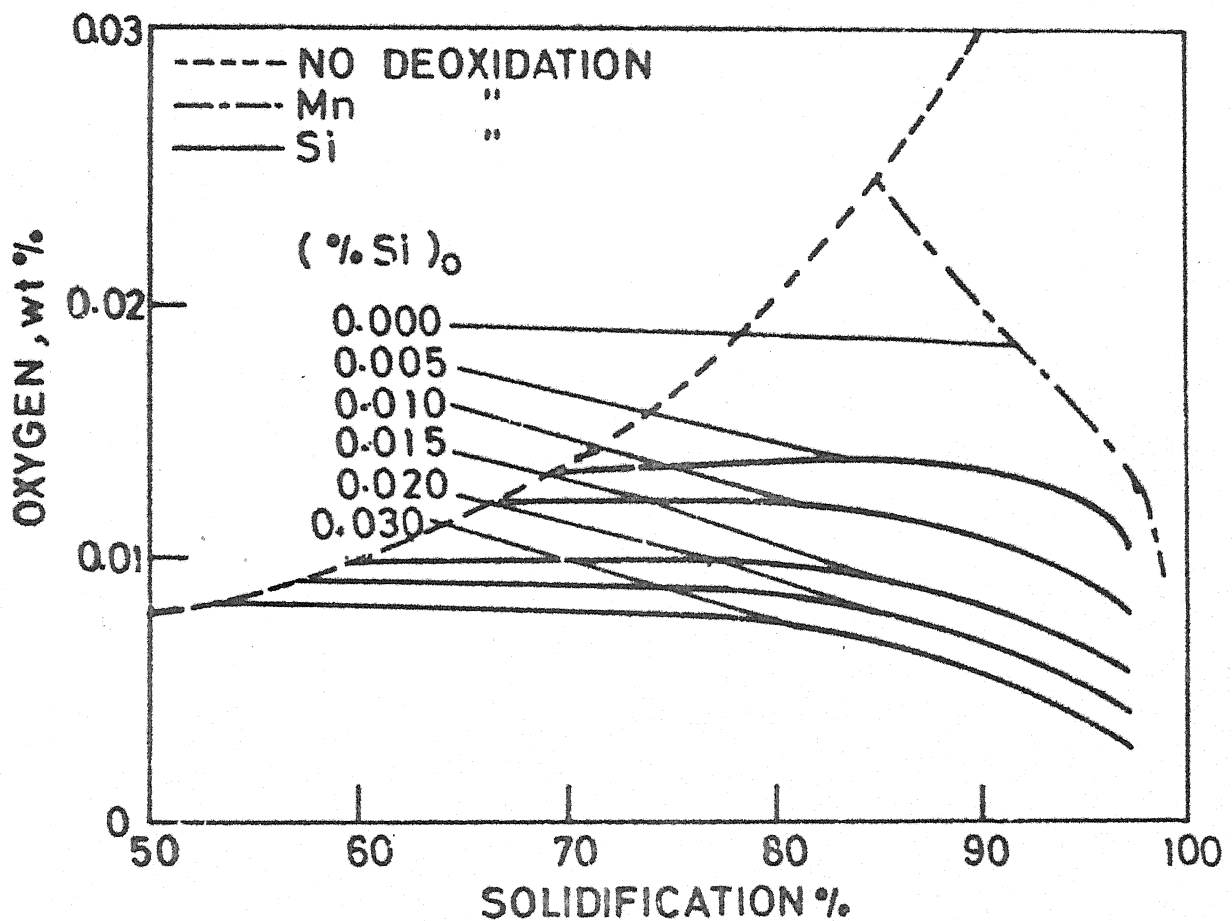
FIG. 1.3   CHANGE IN THE OXYGEN CONTENT
OF ENTRAPPED LIQUID DURING FREE-
ZING OF STEEL (% O)$_0$ = 0.004
(% Mn)$_0$ = 0.50 Freezing temp. = 1525°C

calculating the residual oxygen in liquid at any stage of solidification. Thus for solid silica as deoxidation product, the residual concentration was given by :

$$[\frac{1-g'}{1-g'}, \; c_0 = \frac{32}{28.09} (\frac{1-g'}{1-g'})^{1/3}] \; (c_0)^2 - (c_0)^3 = \frac{32}{28.09} \; \frac{1}{K_{16}}$$

.... (I.15)

where K_{16} is the equilibrium constant defined by the quation

$$[Si] + 2[O] = (SiO_2)(s) \; ; \; K_{16} = \frac{1}{[\% \, Si][\% \, O]} \cdots (I.16)$$

Once the residual oxygen was computed at a particular stage of solidification, and the enriched carbon concentration was known from equation (I.5), the corresponding partial pressure of carbon monoxide could be computed from the equilibrium of the reaction :

$$[C] + [O] = C_0(g) \; ; \; K_{17} = \frac{p_{CO}}{[\% C][\% O]} \; .... \; (I.17)$$

To enumerate the role of carbon in the formation of blowholes, Turkdogan pointed out that for a particular ratio of Si/Mn, and a particular silicon concentration there was a critical carbon content below which carbon-oxygen reaction wouldnot take place, hence no blowhole formation would occur, in the absence of hydrogen and nitrogen. The author' estimation about the critical silicon and carbon contents of 0.5 pct. Mn steel required for the suppression of blowhole formation at 1 atm. CO is shown in figure (I-4).

In the presence of other dissolved gases such as hydrogen and nitrogen, all three gaseous species should be taken to be present in the gas pocket, so that total pressure

$$(P_T) = p_{CO} + p_{H_2} + p_{N_2}$$
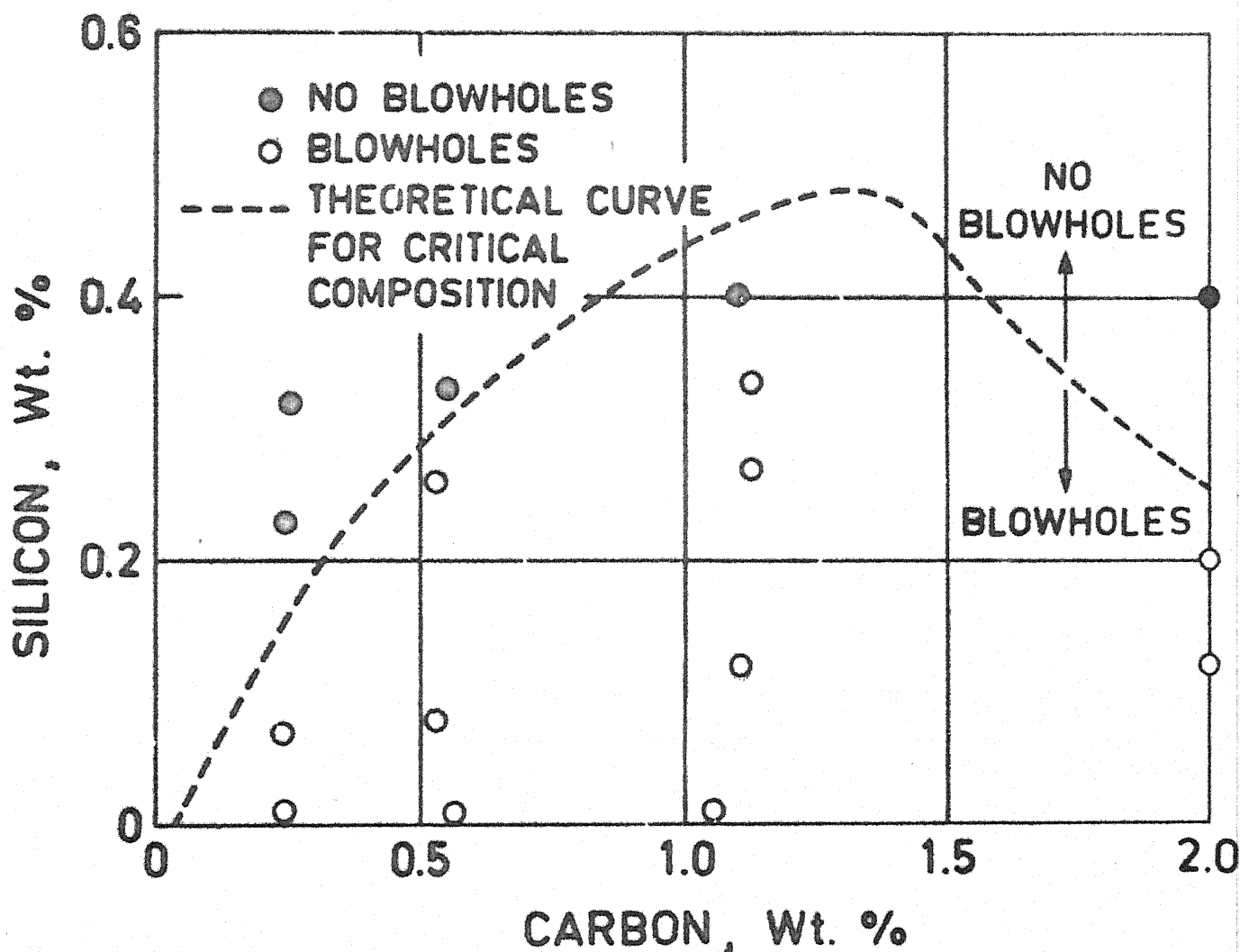
FIG. I.4 ESTIMATED CRITICAL SILICON AND CARBON CONTENT OF 0.5 POT. Mn. STEEL REQUIRED FOR THE SUPPRESSION OF BLOW HOLES 1 ATM. CO[8]

In the theoretical treatment so far discussed a constant freezing temperature was assumed. Such an approximation was reasonable since the impurities concentrations were low.

Harkness, Nicholson and Murray[11] modified Turkdogan's model by considering :

(i)   different partition coefficients for solutes, depending upon whether steel is solidifying to delta (δ) or gamma (γ) phase,

(ii)   variation of the solidification temperature as the solidification proceeds,

(iii)   the effect of solute interactions during gaseous reactions (formation of CO, H_2 and N_2).

(iv)   making the model applicable to a much wider range of composition, then originally proposed by Turkdogan.

(v)   the role of hydrogen and nitrogen in addition to carbon monoxide for the formation of blowholes in steel ingots.

Applying their modified theoretical model to the experimental results, the authors had conclusively proved that means were available for predicting the limits to which various gas forming elements should be controlled to avoid too much porosity in steel ingots. They carried out a large number of experiments in laboratory and plant, and arrived at the conclusion that an ingot with marginal porosity (Fig. I-1) could be obtained if P_T ($= p_{CO} + p_{H_2} + p_{N_2}$) lies between 1 - 1.4 atm. at 90 pct. solidification. If P_T was below that they obtained dense ingots, and at $P_T > 1.4$ atm. ingots with significant porosity. The model was also applied to the production of ladle-balanced steel.

The main gases contributing to blowhole formation in steels are CO, H_2 and N_2 though their relative contribution may vary somewhat. The gas forming reactins are :

(i) $[C] + [O] = CO(g)$; $K_{17} = \dfrac{p_{CO}}{[h_C][h_O]}$,
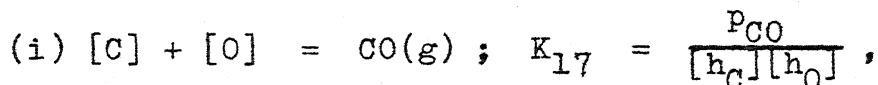
where $h_C = f_C[\text{wt \% C}]$ and $h_O = f_O[\text{wt \% O}]$ ..... (1.18)

(ii) $[H] = \tfrac{1}{2}H_2(g)$; $K_{19} = \dfrac{\sqrt{p_{H_2}}}{[h_H]}$; where $h_H = f_H[\text{wt \% H}]$

..... (1.19)

and (iii) $[N] = \tfrac{1}{2}N_2(g)$; $K_{20} = \dfrac{\sqrt{p_{N_2}}}{[h_N]}$; where $h_N = f_N[\text{wt \% N}]$

..... (I.20)
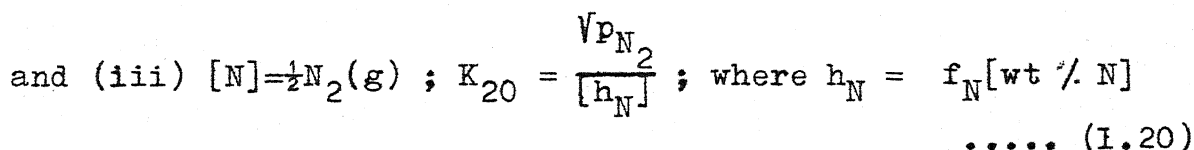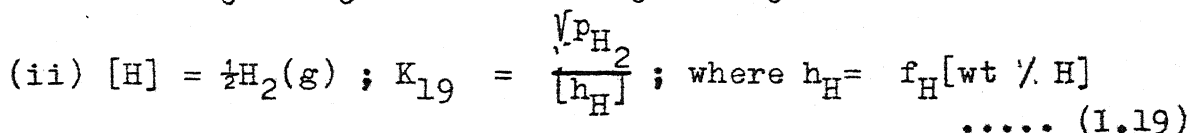
Examples of how p_{CO}, p_{H_2} and p_{N_2} can contribute to P_{Total} is given in fig.(I-5). It is apparant that the relative contribution of the gases change during the solidification process. In the early stages of solidification p_{CO} tends to dominate, but towards the end of solidification the combination of p_{H_2} and p_{N_2} eventually makes the larger contribution to P_{Total}.

The authors conclusion about the pressure criterion (i.e., 1-1.4 atm.) for ingots with marginal porosity is expected because when the ingots are marginally porous, that is when the blowholes originate at top head of the ingot (approximately around 90 pct. solidification), ferrostatic pressure is close to zero and in such a case the thermodynamic pressure is approximately equal to the atmospheric pressure (i.e. one atm.) or slightly higher.
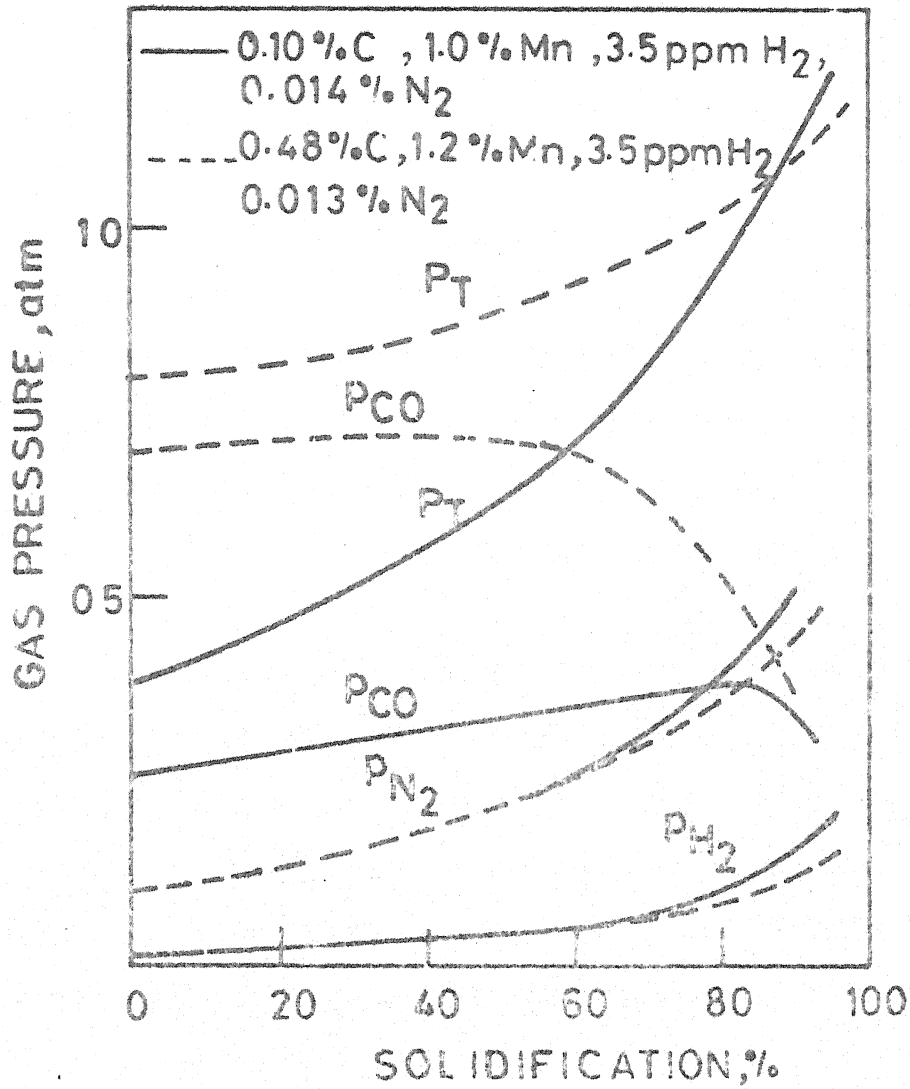
FIG. I.5 EXAMPLES OF CONTRIBUTION OF P_{CO}, P_{H_2} AND P_{N_2} to p_T^{11}
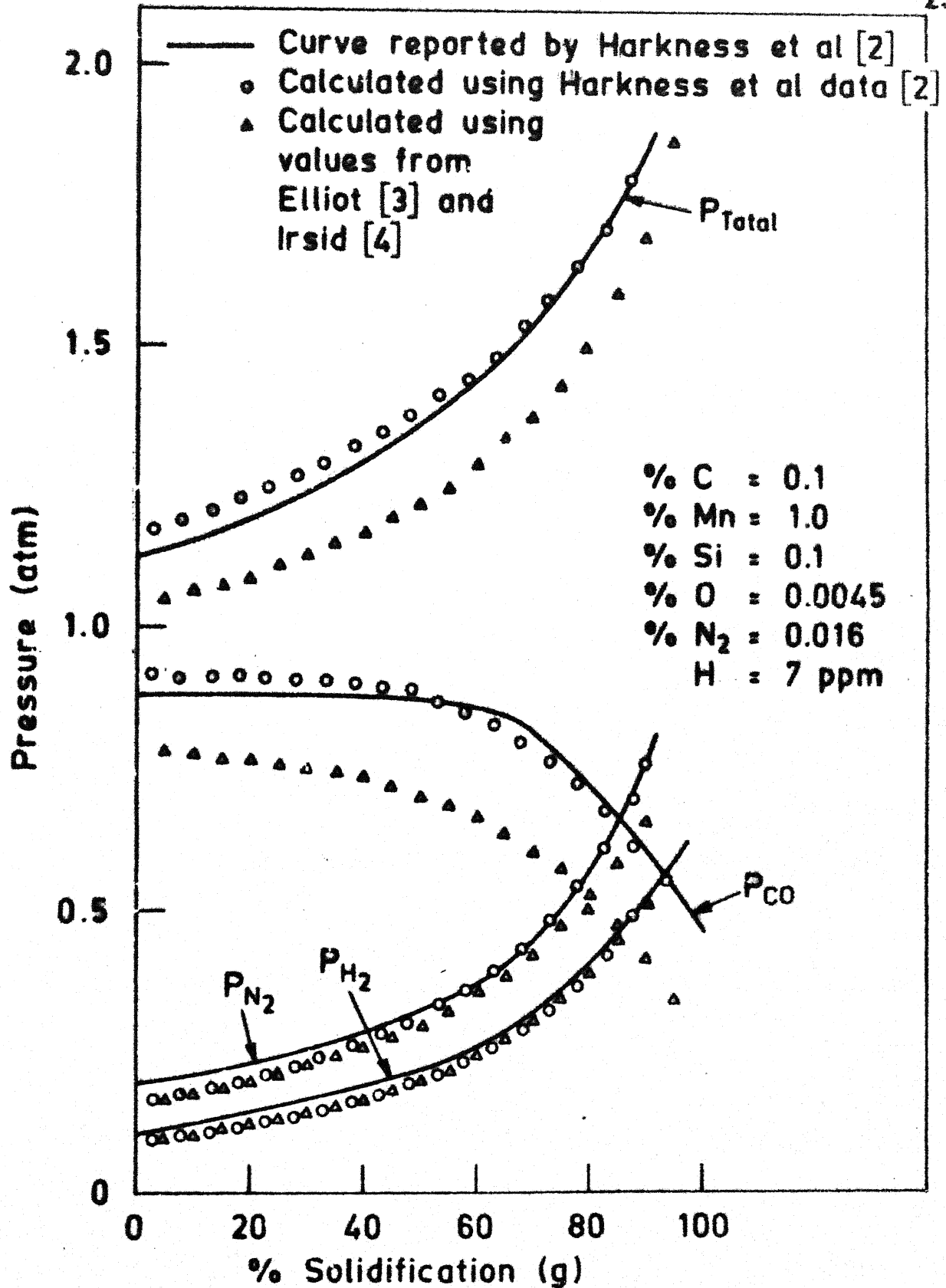
Fig. I.6 Variation of partial pressure of CO, H_2, N_2 and total pressure $(P_{CO} + P_{H_2} + P_{N_2})$ with increasing solidification for low carbon steel.
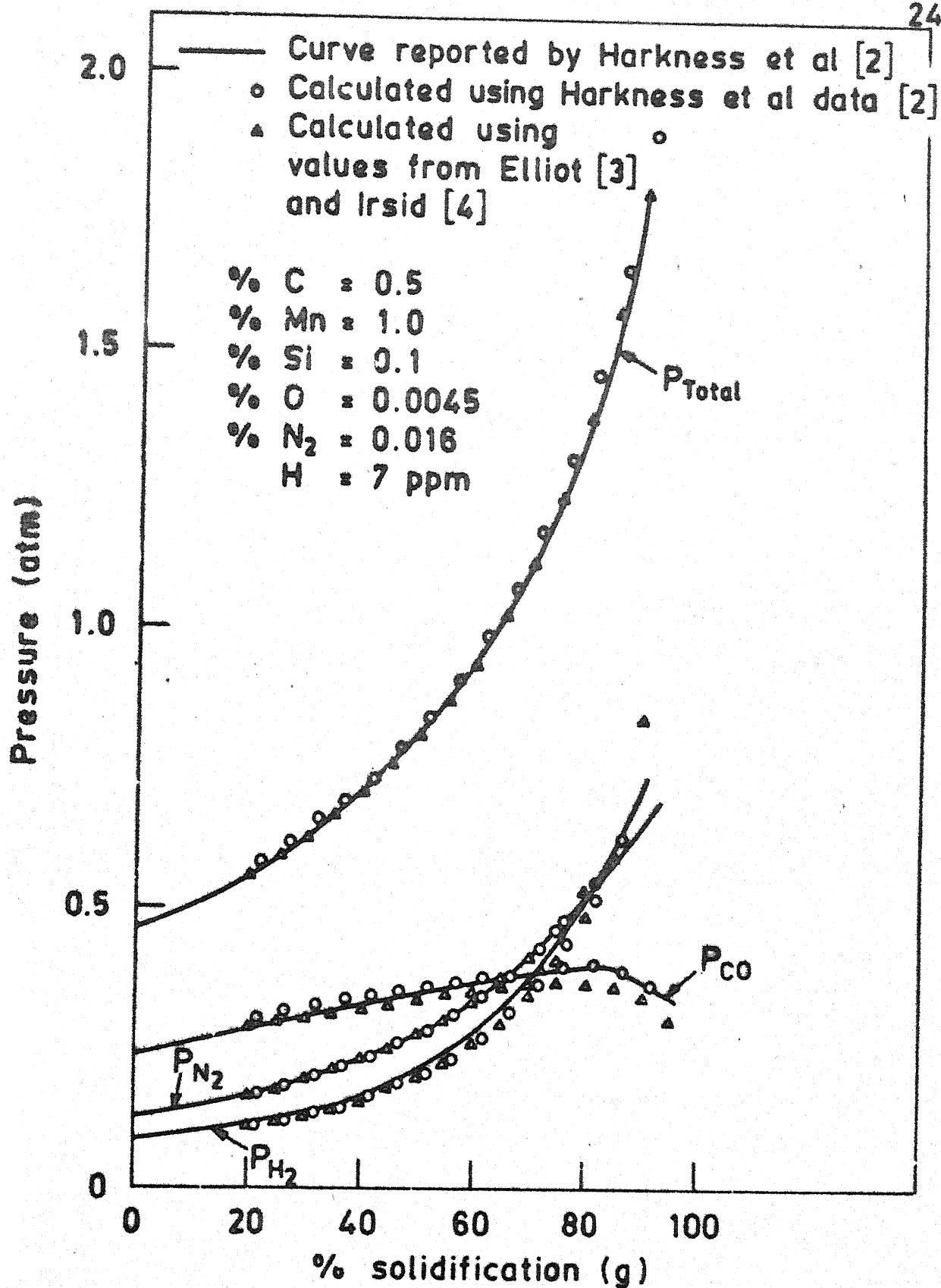
Fig. I.7 Variation of partial pressure of CO , H_2 , N_2 and total pressure ($P_{CO} + P_{H_2} + P_{N_2}$) with increasing solidification for high carbon steel.

of both Turkdogan and Harkness et al was the assumption of complete macromixing in liquid which went unstated.

The work of Harkness et al[11] high lighted role of CO, H_2 and N_2 in the formation of blowholes in steel ingots, when the state of oxidation is high in the steel, then only small amounts of hydrogen and nitrogen are required to produce blowholes and the contribution of p_{CO} to P_{Total} is large. However when the state of oxidation is low, blowholes form only when hydrogen and nitrogen levels are high and p_{H_2} and p_{N_2} make the major contribution to P_{Total}.

Following the model of Harkness et al, Bagaria and Brahmadeo[12] had developed a computer programme for the calculation of gas pressure at various stages of solidification. The programme has been tested for low carbon and high carbon steels and the comparison with values reported by Harkness et al shows that the agreement is within 5 pct. This is shown in figs. (I-6) and (I-7).

I.3   PLAN OF WORK

The objective of the present investigation is to produce semi-killed steel ingots in the laboratory to test the emperical findings of Harkness et al[11].

The detailed plan is noted below :

(i)   selection of composition for steel melting in the laboratory induction furnace,

(ii)   melting of steel in induction furnace under controlled atmosphere,

(iii)   deoxidation of the steel bath with ferromanganese and ferrosilicon,

(iv)   measurements of temperature,dissolved oxygen in molten steel,

(v)   sampling by aspiration technique in the furnace as well as in the mould,

(vi)   chemical analysis of the meltdown composition by wet chemical as well as by spectroscopic method,

(vii)   calculation of gas pressure at 90 pct. solidification from the data obtained using the computer programme developed by Bagaria and Brahmadeo[12],

(viii)   prediction of ingot structure (highly porous/marginally porous/dense) based on emperical findings,

(ix)   longitudinal sectioning of the cast ingots and measurement/visual abservation of the extent of porosity,

(x)   establishment of agreement/disagreement between (viii) and (ix),

(xi)   theoretical computation for Si-Mn-O equilibrium from the data available from (iv) and (vi),

(xii)   SEM and EPMA of the inclusions from selected region of the ingot,

and (xiii)establishment of agreement/disagreement between (xi) and (xii).

CHAPTER   II

EXPERIMENTAL

The discussions in this chapter may be convini-
ently split down into the following :

- Preliminary requirements
- Experimental set-up for the production of st-
  eel ingots
- Auxilliary measurements
- Experimental procedure.

II.1   PRELIMINARY REQUIREMENTS

II.1.1   Selection of compositions for experiments :

Based on the value of total gas pressure $P_T (= P_{CO} + P_{H_2} + P_{N_2})$ desired at 90 pct. solidification, the compositions
were selected. A total pressure range from around 0.8 atmos-
phere to 1.4 atmosphere were considered for this purpose.
The computer programme which calculates the gas pressure as
a function of percentage solidification from the initial ba-
th compolition, includes six distinct input variables e,g
wt.pct.O, wt.pct.Si, wt.pct.Mn, wt.pct.C, wt.pct.N and H(ppm).
The first three of the six variables were obtained from a
seperate computer programme[13], which gave the quilibrium oxy-
gen content for a wide range of manganese and silicon content
of the bath.

Mn-Si-O equilibrium calculations were done for three distinct temperatures, 1550°C, 1600°C and 1650°C. Since the present investigation was intended to restrict over low carbon range only, the computer programmes were run for wt.pct.C varying between 0.1 to 0.15. However possible ranges of nitrogen and hydrogen contents were picked up from the literature[11]. The values obtained from Mn-Si-O equilibrium were next coupled with the values of C,N and H for each temperature. The all possible combinations were next fed into the computer programme[12] and those compositions were only selected which gave a total gas pressure P_T between 0.8 atmosphere to 1.40 atmosphere at 90 pct. solidification. The selected compositions were next tabulated for three different temperature values. Moreover, simultaneous calculations were done to record the amount of manganese, silicon and carbon to be added to the 8 kg. steel bath.

II.1.2   Preparation of charge

Mild steel rounds (0.26 pct. C, 0.16 pct. Si, 0.70 pct. Mn) were obtained from TISCO. The rounds were initially cut off to a size of 1 to 1.5 meters. These were later cut into pieces of around 6 to 8 Cm. size with the power saw. The pieces were next treated in a solution of dilute sulphuric acid for around 6 hours, then they were thoroughly cleaned with water, dried with acetone and preserved in an air tight polythene bag. Around 8 kg. of clean and dry mild-steel rounds were fed as charge into the induction furnace for each heat.

II.1.3   Preparation of deoxidisers and other additives :

The deoxidisers used were primarily ferromanganese (59.5 pct. manganese) and ferrosilicon (94.7 pct. silicon). Besides these, carbon as graphite was one of the necessary additives in each heat. Prior to their use, the compositions of the deoxidisers had been determined by the wet chemical methods. The deoxidisers available in the form of lumps were ground to a moderate size (around 10-20 mesh) with the help of a hammer. The ground deoxidisers were dried in an oven for 48 hours at a temperature close to 120°C, and were finally preserved in dessicators. Analogous treatment was given to graphite also.

II.1.4   Preparation of crucible :

The crucibles were made insitu using dead burnt magnesite (source:Almora,U.P.). Prior to these sets of experiments, several preliminary trials runs were conducted and in the course of it the quality and quantity of material together with the method of fabrication of magnesite crucible were assertained. The raw material includes :

Dead burnt magnesite	30 pct.	—	-30 mesh
	30 pct.	—	-60 mesh
	40 pct.	—	-100mesh
Silica (white foundry sand)	5 pct.	—	-100mesh
Magnesium chloride (Laboratory Reagent)	6 pct.	—	—
Borax (Laboratory Reagent)	0.1 pct.	—	—

The fabrication procedure is outlined below in nutshell. The raw magnesite was forst ground and then screened to yield the above size fractions. Around 8 kg. of dead burnt magnesite was needed to prepare one crucible for the induction furnace. The magnesite, silica and borax powders as per above specification were dry mixed for about 30 - 40 mts. in automatic mix muller.

6 pct. magnesium chloride (480 grams for 8 kg. magnesite) was dissolved in one lit. of water had been found optimum for getting dense ramming[14]. The magnesium chloride solution was added slowly in muller and mixed in muller for about 30 - 40 mts. The thoroughly mixed magnesite, silica,borax and magnesium chloride with water was taken out of the muller and used for ramming.

Figure II.1 illustrates the induction coilmica sheet and graphite mandrel assembly. Before ramming, two thick mica sheets were put around the inner periphery of the coil. The space in between was filled with alumina powders. The bottom of the cavity was rammed first and then a tappered graphite mandrel, covered with a piece of paper was put into the cavity. This mandrel and the inner mica sheet. The ramming mixture was put into this gap and spread uniformly and rammed using ramming rods. As the ramming proceeded, the material went deep inside and fresh mixture was put. This was repeated for a number of times till the lining was brought upto the top of the coil. Care was taken to achieve maximum density and uniform thickness for the crucible. Then the
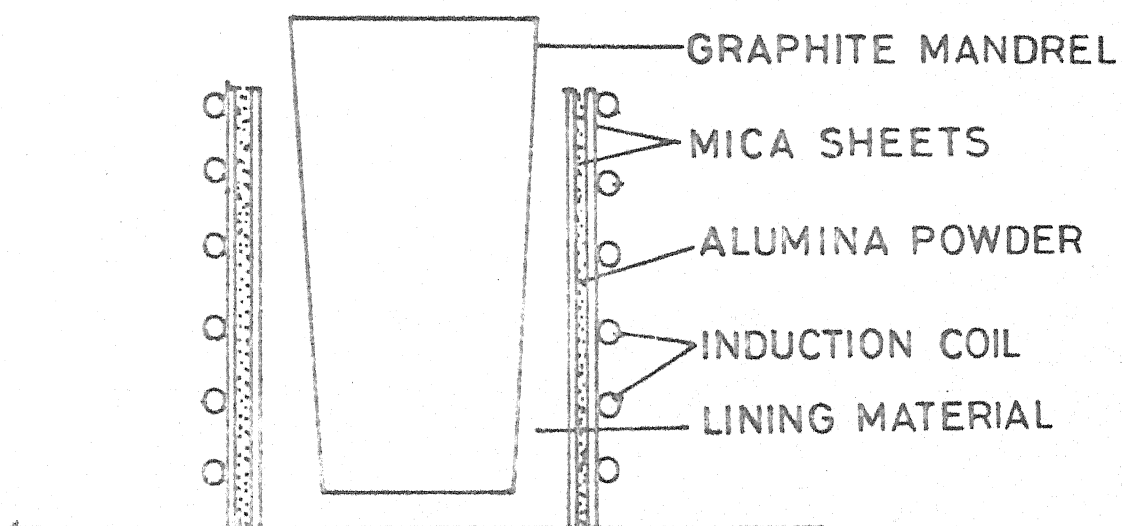
FIG. II.1   INDUCTION COIL, MICA SHEET AND
GRAPHITE MANDREL ASSEMBLY

graphite mandrel was removed and the crucible was checked
from inside before sintering. Any gap left were set alri-
ght by filling it with the mixture. The whole assembly was
allowed to dry for 24 - 36 hours. Then the mandrel (without
paper) was put back for the purpose of sintering.

Figure(II.2) schematically shows the graphite man-
drel. There are a number of holes on the mandrel, drilled
from surface to the axis and the central axial hole connects
all other surface holes. This arrangement was provided for
easy exit of gases during sintering and avoiding the excess
gas pressure on any part of the crucible. Sintering was
done to get as dense and impervious crucible as possible.
It was carried out in two stages, first at a relatively
low temperature (600 - 800°C) and then at a sufficiently
high temperature (1500° - 1600°C). After sintering the cru-
cible was checked from inside for any type of defects and
cracks. If there was any such defect, fresh, relatively di-
lute ramming mixture was used for patching up.

In the initial stage of experiment, it was recogn-
ised that the crucible life was relatively poor (around 1 to
2 meltings). This inturn imposed a restriction on the pace of
the work because the entire process of crucible making was
time consuming. This called for an improvement of the crucible
life and for this necessary consultations were done with others[15].
It was found that the life can be substantially increased by
incorporating much more finer fraction of magnesite instead of
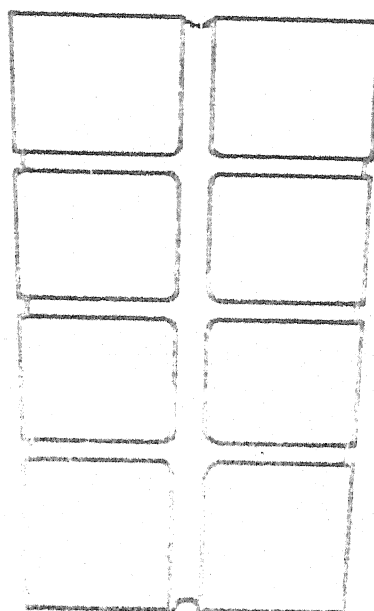
FIG.II.2 GRAPHITE MANDREL

coarser fraction in the ramming mixture. Hence the size distribution of dead brunt magnesite was decided as :

Dead burnt magnesite 30 pct. - -35mesh

30 pct. - -65mesh

40 pct. - -200mesh

With the above modification in the size distribution of dead burnt magnesite, improvement in the crucible life was obtained. On an average a crucible then lasted for about 5 meltings. It should be possible to improve it further. But the performance was felt to be satisfactory.

II.1.5 Preparation for sampling at various stages of the experiment :

Sampling was carried out at three stages e,g

a) suction sampling of the melt, just after the addition of the deoxidisers to determine the total oxygen content in the melt.

b) copper mould sampling to determine the bath composition of molten steel for C,Si and Mn.

c) suction sampling of the metal in the mould to determine the level of total oxygen picked up during pouring.

Figure (II.3) schematically shows a suction sampler. Silica tube of internal diameter 5 mm was fitted to a rubber bulb for taking the suction samples. The silica tubes had been washed with concentrated acid and then with water and then were dried in oven before being attached to rubber bulb. The silica tubes were flushed with a mixture of nitrogen and argon gas to
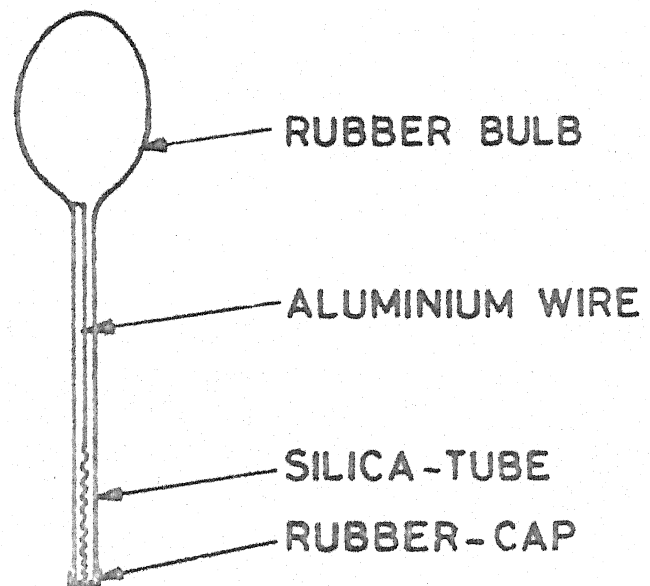
FIG.II.3 A TYPICAL SUCTION SAMPLER

ensure that an appreciable quantity of oxygen doesnot remain inside the tube. The tubes were next closed with an air tight cap, so that leakage is minimised. In addition to this, a thin coiled wire of pure aluminium was kept inside the tube with the purpose of obtaining a dense sample.

Figure (II.4) schematically shows the copper mould, which is a massive block of copper containing a central cylindrical groove. The sample in the form of a tiny ingot was subsequently taken for spectroscopic and wet chemical analysis. Some aluminium chips were kept in the copper mould for deoxidation, so that a dense sample is obtained.

II.2   EXPERIMENTAL SET UP FOR THE PRODUCTION OF STEEL
        INGOTS

II.2.1   The induction furnace

The 20 kw Ajax Northrup Converter (make, Ajax magnethermic corporation, New Gersy, USA) is a frequency changer designed to convert 50 c/s power supply to a high frequency one of approximately 20,000 c/s. The frequency range delivered by the converter will vary usually from about 12000 to 35,000 c/s depending upon the size of the coil connected to the converter and the load in the furnace.

The converter consists essentially of a high voltage transformer, a mercury arc spark gap, capacitors and an induction coil. The spark gap contains two electrodes, a pool of mercury and means of controlling the level of the mercury in a manner
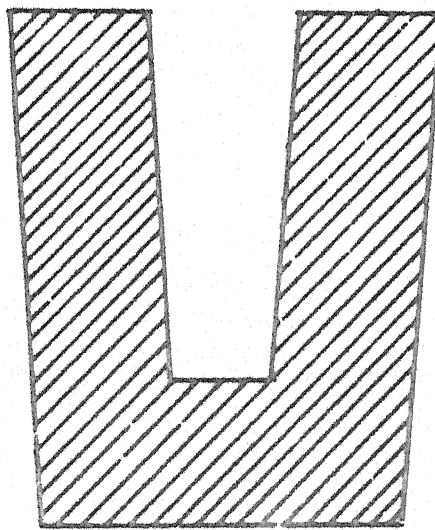
FIG. II.4 THE COPPER MOULD

which will allow the mercury pool level to be adjusted from
a position where the electrodes touch the mercury to a posi-
tion with a space of about 2 Cm. between the tip of the
electrodes and the mercury pool.

The transformer is designed with an internal reac-
tance which will limit the current drawn when short-circuited,
to about 86 percent of full load.

The capacitors are charged by the high-voltage tran-
sformer untill they have sufficient charge to cause a breakdown
or arc to occur between the mercury pool and electrodes. This
then sets up a high frequency alternating current which flows
through the induction coil.

The melting furnace consist of a hollow induction
coil made of copper tubing, through which is passed for coo-
ling the mica lining and the refractory lining (Rammed magne-
site in this case) for holding the liquid metal. The induction
coil is assembled in a non-metallic frame consisting of asbest-
os cement which sits on a convinient table with contact wells
in the table top. This contact wells contain about 2.5 Cm. of
mercury which permits a good electrical connection to be main-
tained between the furnace terminals and the power leads atta-
ched to the contact wells on the other side of the table.
Heating and melting of the metal is accomplished by filling
the space in the refractory lining with small pieees of metals.
High frequency eddy currents are induced in the metal pieces
near their surface which cause them to become hot and melt.

II.2.2   Earlier trials on steelmelting:

A number of trials were conducted prior to this set of experiment in order to create a proper experimental condition. The earlier investigations[16] were aimed at :

a)   checking the reliability and response of various equipments used in the process, as for example immersion oxygen probe. Intrials the oxygen content of the bath as given by the immersion probes were found to be in reasonably good agreement with the actual oxygen content of the bath.

b)   evaluating the performance of insitu magnesite crucibles.

In the initial stages of the trials, melting as well as casting were normally done in air. However this had a serious adverse effect upon the entire operation, because :

a)   the melt oxygen content was too high. Oxygen probe data showed upto 1400 ppm oxygen at $1600^{\circ}C$ under normal air melting.

b)   formation of a huge amount of iron oxide, which necessitated deslagging. Moreover the solid crust of iron oxide formed on the top of melt, where a relatively low temperature prevails (Temperature in the furnace is not uniform but increases downwards) posed a serious difficulty in suction sampling.

c)   owing to quite high oxygen content of the melt, the suction samples obtained were porous in majority of the cases and hence were to be discarded, since no fruitful analysis could be carried out on porous samples.

d)   since the meltdown time was different from
heat to heat, (the aspect being related to the power fed to
the furnace and which kept on varying from time to time), it
became very difficult to ascertain the level of initial oxygen
in the bath. Unless an approximate value of initial oxygen is
known, the necessary amount of deoxidisers to be added to yi-
eld a particular end oxygen content in the bath can't be cal-
culated.

Thus it became necessary to introduce certain modi-
fication as well as improvements upon the existing fascilities,
so that experiments could be conducted under controlled condit-
ions. These are discussed below in section II.2.3 and II.2.4.

II.2.3   Continuous inert gas flushing in the furnace chamber :

Figure (II.5) shows the inert gas flushing arrangements
in the furnace. The furnace was open at its mouth, through which
continuous transfer of oxygen occured from the atmosphere to the
melt. To minimise oxygen pick up during melting a refractory top
was made to cover the mouth. The top had a circular aperture of
around 10 Cm. diameter. The aperature was closed with a refract-
ory plug, which had a central hole of around 0.6 to 0.7 Cm.
Through this hole a silica tube was introduced down to the metal
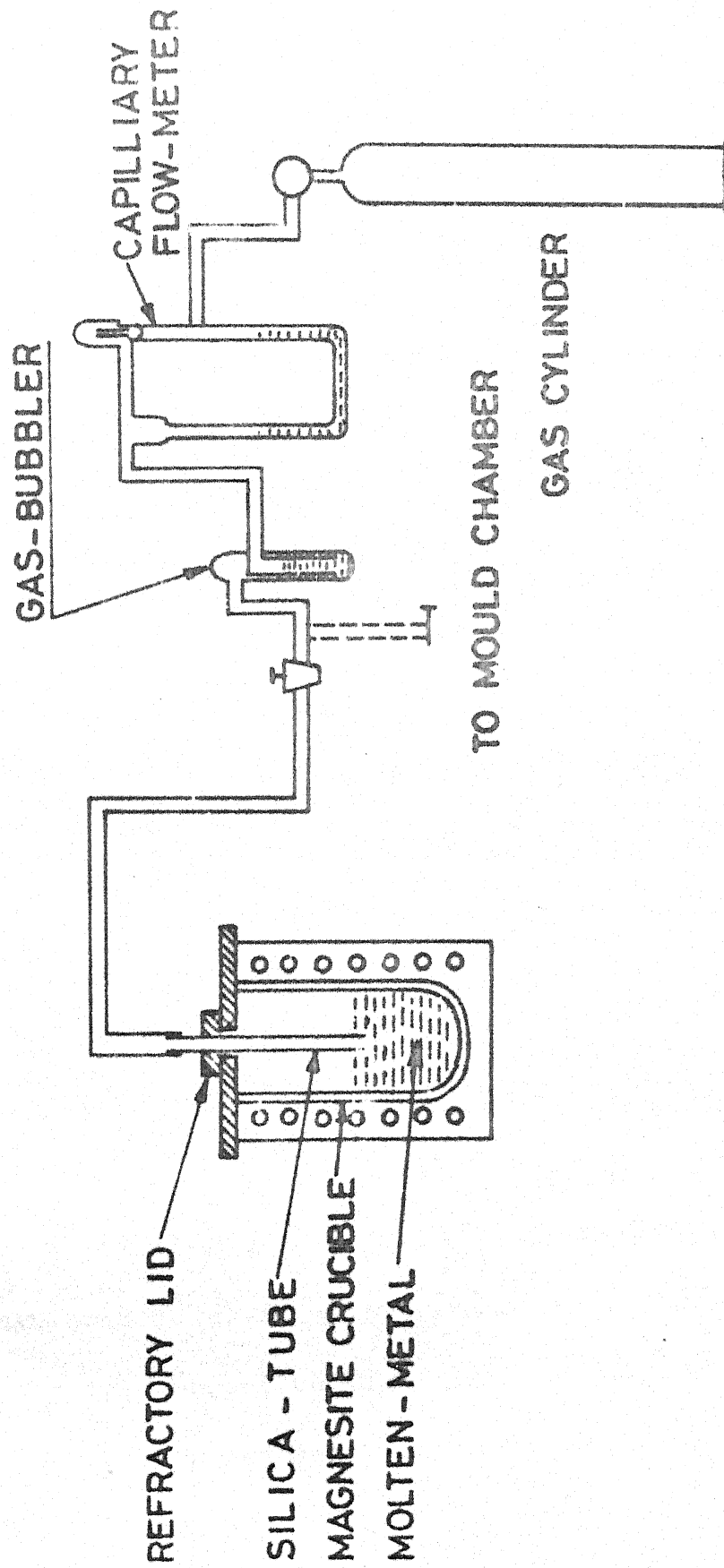
FIG. II.5   INERT GAS FLUSHING ARRANGEMENTS
IN THE FURNACE

level. The other end of the silica tube was connected to the inert gas cylinders (nitrogen and argon gas) through tubes, stop cocks and flowmeters. Throughout the experiment inert gas at a rate of around 1 lit./min. was flushed into the furnace.

In the course of experiments, during addition of deoxidisers, suction sampling as well as during immersing the oxygen probe, the refractory plug together with silica tube were removed temporarily and then replaced again. As the metal pool height kept on decreasing with progressive melting of the charge, the silica tube height was also adjusted accordingly.

II.2.4   Casting under inert atmosphere

Figure(II.6) shows the arrangement for casting under inert atmosphere. This was done with a view to minimise the extent of gas pickup upon pouring. The mould was kept in a rectangular mild steel container, which was specially fabricated for this objective. The container, made of two distinct halves was fabricated upto such a height, that when the furnace was tilted for poouring, the tip of the lip of the crucible almost touched the top opening of the container. Thus the length of the pouring stream exposed to the atmosphere was very small.

RUBBER CAP

EVACUATED
MOULD CHAMBER

MOULD

SAND - BED

PRESSURE TUBES

TO INERT GAS
CYLINDERS

THREE-WAY
VALVE
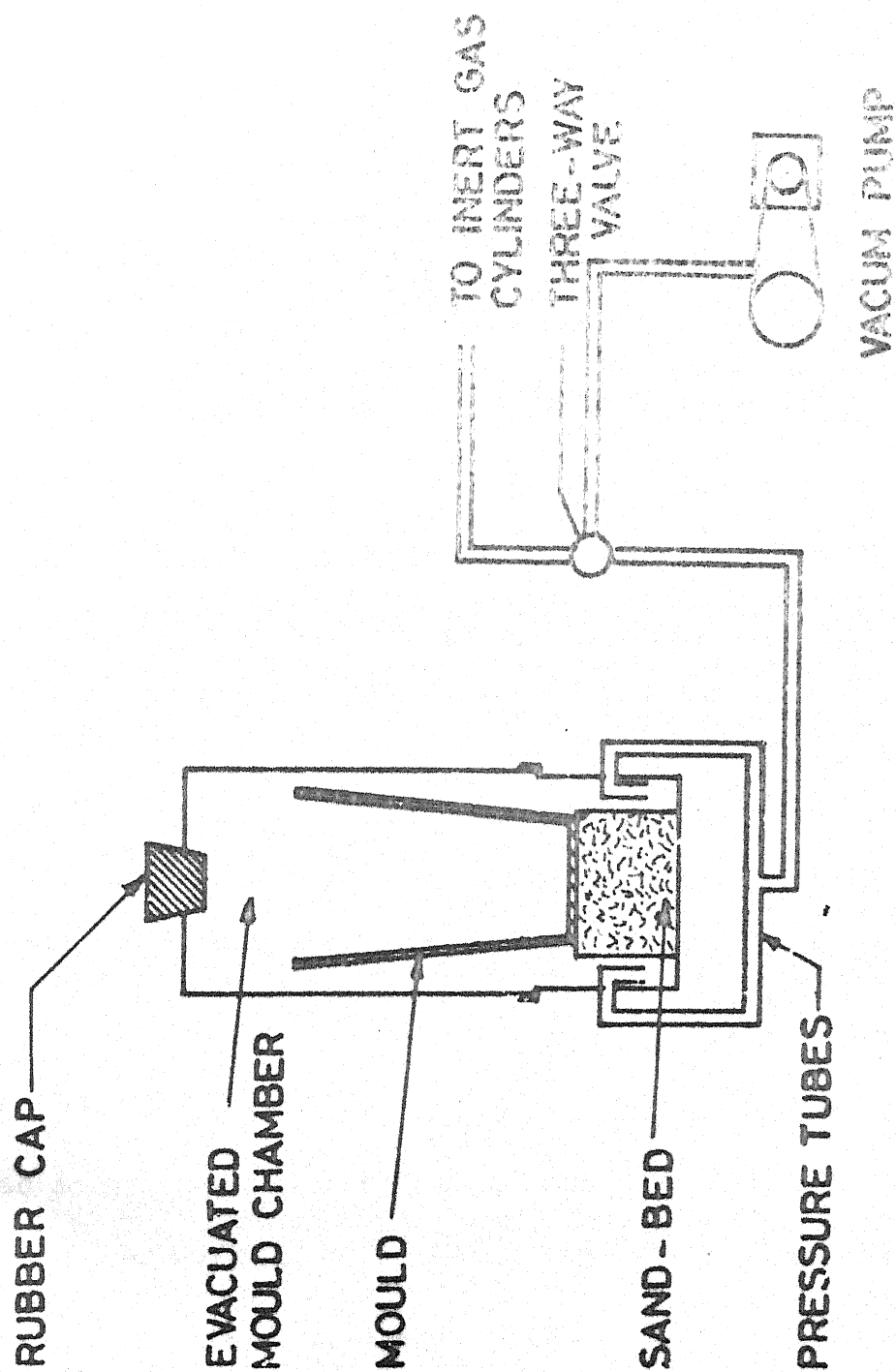
VACUM PUMP

FIG. II.6   CASTING UNDER INERT ATMOSPHERE
DURING THE EXPERIMENT

Besides the top central opening, there were two openings on either side of the lower half, which were connected by tubes through stop-cocks to the vacuum pump and the inert gas cylinders. Arrangements were also there to raise the mould height almost upto the top opening of the container. To minimise leakage, a groove set on the lower half of the container was filled thoroughly with plasticine . After the mould was placed in the proper position, the upper half was placed on the groove and forced deep into the plasticine. Once the mould was enclosed, the top opening was closed with a rubber plug and the evacuation of the chamber was carried out to thepoint, till the manometer showed a pressure of around 4 to 5 mm. The stopcock was next turned in such a way that both the outlets of the container remain closed and vacuum maintained. At a latter stage of experiment, the stopcock was again rotated and inert gas mixture was fed into the container till it was completely filled up. During pouring the top rubber plug was removed and metal was poured into the mould.

II.3   AUXILLIARY   MEASUREMENTS

II.3.1   Measurement of bath temperature with thermocouple :

It was necessary to know the approximate bath tem-
perature at the melt down because the amount of deoxidisers
to be added could only be found out once the temperature
known approximately. Pt/Pt-10 pct. Rh thermo couple was used
to obtain the bath temperature. The thermo-couple ends were
connected to a digital milivoltmeter (make, Televista (New
Delhi, India) through compensating lead wires. The thermo
couple tip was covered with a layer of high temperature alu-
mina cement to protect the junction from the high temperature
of the molten metal.

Heat transfer calculations were carried out to find
out the time of immersion required. It was calculated that for
a spherical geometry of the alumina cement coating of 0.5 Cm.
diameter, it would approximately give the bath temperature in
about 4 seconds time of immersion.

The alumina cement coating was dried thoroughly
before the thermo couple was dipped into molten steel. From
the E.M.F. as displayed by the milivoltmeter, the temperature
of the bath was found out from the standard Pt/Pt-10 pct. Rh
thermo couple chart, after incorporating necessary room tempe-
rature correction.

II.3.2   Measurement of dissolved oxygen as well as

           bath temperature by immersion oxygen probe.

The probes used for the investigation were the 'cellox II probes' (make Electronite, Belgium). The immersion oxygen probes are the example of typical technological application of solid electrolytes. The cellox II is basically composed of a solid zirconium oxide cell for measuring oxygen activity, and a Pt/Pt-10 pct. Rh thermocouple for measuring temperature simultaneously. Some of the charateristics of cellox II probes are high-lighted below :

Temperature range : $1250^{\circ}C$ - $1750^{\circ}C$

Thermo couple   :   Pt/Pt-10 pct. Rh

Oxygen range   :   -200 to 300 mv.

Accuracy   :   Approximately .5 pct. of

                              the whole of the range.

The electrochemical cell which make up the oxygen measurement tip is :

$$M_o/Cr + Cr_2O_3// \; ZrO_2(MgO) \; // \; a(O)_{Fe}/Fe$$
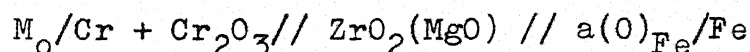
in which

M_o = The molybdenum negetive electrode wire of the reference side

$Cr+Cr_2O_3$ = chromium-chromium oxide serving as oxygen reference.

$ZrO_2(MgO)$= solid electrolyte or zirconium cell, magnesia stabilised

$a(O)_{Fe}$ = oxygen activity in liquid steel bath, to

Fe   = positive iron electrode in contact with steel

The relationship between oxygen activity, EMF and temperature for the cellox II with reference Cr/Cr_2O_3 is given by the following equation·

$$\log_{10} a(O) = 1.36 + 0.0059 \; [\; E + 0.54 \; (t^o - 1550)$$
$$+ 2 \times 10^{-4} \times E \; (t^o - 1550) \quad \ldots \; (2.1)$$

The cellox II probe was introduced into the bath by means of lance which is composed of contact block, a lance holder, a steel tube, a copper clad ceramic insulated inside lead, a handle, a fast connector and an outside lead.

The four terminals coming out of the lance is next connected to a dual pen voltage-time recorder (Make Digital Electronics Ltd.Bombay) which records the E.M.F. given by the cell as well as by the thermo couple as a function of time. On an average 10 seconds time was needed to obtain a stable EMF, and thus the probe was to be kept immersed into the bath for atleast 10-12 seconds.

II.3.3   Measurement of total oxygen content by Leco-oxygen
          determinator:

Total oxygen (oxygen present in the dissolved state plus the oxygen present as combined oxides) content of the suction samples were determined by oxygen determinator (make Leco corporation, USA).

The determinator has two parts viz. the EF-10 Electrode furnace (model 777-100) and the RO-18 oxygen determinator (model 775-300, 775-400 (BCD)). The Leco RO-18 oxygen determinator, determines oxygen in steels,iron, nonferrous metals and inorganic substances. The RO-18 uses the inert gas fusion method. The EF-10 electrode furnace is designed for fusion analysis method. A graphite crucible, held between two

water cooled metal electrodes, reaches temperature near 2700°C. The   matic closing system of the electrodes offers the best possible crucible contact for high current fusion. At this high temperature the sample gets fused and all the oxygen released as carbon-monoxide, which is carried by the carrier gas (ultrapure argon) to the RO-18 for measurement by in rared detection. The detector output is amplified, linearised, inte- rated and displayed directly as percentage oxygen.

The RO-18 is equipped with automatic sequence for more operator convinience and speed. The RO-18 contains a gas doser for theortical gas dosing for quick and accurate calibration.

Prior to the actual analysis of the samples it is necessary to calibrate the instrument and adjust the blank. Calibration is done with the leco standards. Calibration is completed when the display shows a percentage oxygen, which corrsponds to the actual oxygen content of the : eco-standards. The black adjustment becomes necessary because the atmosphere inside the furnace may introduce significant error in the final result.

The characteristics of the determinator are as noted below :

Range   : Low range   .0001 pct. (sample weight 0.8 to 1.199 gm) to .1000 pct. (sample wt. 0.8 to 1.199 gm)

High range   .01 pct. (sample weight 0.4 to 1.0gm) to .20 pct. (sample weight 0.4 gm. max

Accuracy : Low range ± .0002 pct. or ± 1 pct.

of oxygen content which-

ever is greater

High range ± .10 pct. or ± 1 pct. of

oxygen content whichever

is greater

Sensitivity: .0001 pct (1 ppm)

Carrier gas: Argon

Purity : 99.95 pct. minimum

II.3.4 Analysis of the melt-down composition.

For wet chemical analysis the turnings of copper

mould sample were used. The analysis was carried out in the

analytical laboratory, Metallurgical Engineering Department,

I.I.T.,Kanpur. The samples were analysed for carbon, silicon

and manganese. Standard procedures were adopted in each case.

Carbon was determined by ohlein's apparatus, manganese by

photomet method and silicon by gravimetric method. The

accuracy in each of these cases are[17].

Strohlien's apparatus ± .02 for carbon

Photometric method ± .02 to ± .03 for manganese

Gravimetric method ± .03 to ± .03 for silicon

Spectroscopic analysis was also carried in the Field

gin factory, Kanpur. Disc type pieces were prepared from the

copper mould sample, and the analysis was done by Quantovac.

The spectroscopic analysis were carried out with the objective to cross check the result of the wet chemical analysis. This will be discussed latter.

II.3.5   Determination of nitrogen content in suction samples:

The analysis of nitrogen was also carried out in the Field gun factory, Kanpur by the inert gas fusion apparatus. The principle of analysis is same as that outlined in section II.3.3 for oxygen determination

II.3.6   Measurement of temperature and relative humidity
          to record the experimental condition :

Since estimation of actual hydrogen content in steel was not possible, the values of vapour pressure of moisture in atmosphere were used to infer the approximate hydrogen content in steel. This will be discussed later.

For this purpose, in every experiment the average relative humidity and average room temperature were recorded with the help of a hygrometer (Make Barigo, Germany) and a thermometer. The hygrometer and the thermometer data were subsequently used to determine the vapour pressure of water from standard Engineering handbooks.

II.4   EXPERIMENTAL PROCEDURE

Around 8 kg. of mild steel was used as charge of the induction furnace. The mild steel pieces were stacked properly in the furnace to obtain as close a packing as

possible . The furnace opening was then closed and the power turned on. For some initial period of time, power was kept at 5 KW, which then was gradually increased upto 15-16 KW. Right from the begining the furnace chamber was continuously fleshed with the inert gas mixture. Simultaneously, the mould was set in the rectangular container and the vacuum pump put on to evacuate the mould chamber. Meanwhile the oxygen probe was fitted with the lance and connected to the dual pen voltage, time recorder. The recorder was already connected to the power source, so that it became stabilise by the time when oxygen probe was to be immersed.

Three compositions were selected each at 1550°C, 1600°C and 1650°C. A table was prepared which recorded the amount of deoxidiser to be added against each temperature, to achieve a specific composition. Corresponding to three temperatures, weighted amount of ferromanganese, ferrosilicon and carbon were kept in containers. On an average the meltdown time was around 3 hrs. This ofcourse was a function of the power rating of the converter.

Once the charge was completely molten, visual observation was made to approximate the bath temperature and to see whether slag etc. was floating on the top of molten metal. Once the metal was sufficiently fluid, deslagging was carried out and then the thermo couple was immersed into the bath. Enough care was taken to see that the power was being put off for a short while at this stage. The bath temperature was calculated from the E.M.F. instantaneously and corresponding amount of ferro-

manganese, ferrosilicon and carbon were then added to the bath. If the temperature of the bath was found to be on the lower side, power was increased to increase the melt temperature. However previous trials on induction furnace had shown that for a power rating of 16 KW, approximately $1600^\circ C$ bath temperature was achieved.

Measured amount of deoxidisers were added in two stages and a mixing time of around 2 min. were allowed for homogenisation of the bath. Then suction sampling was carried out and the samples after being quenched in water, were preserved for subsequent analysis.

After suction sampling was over and the sample looked satisfactory, the power was put off and the probe was immersed into the pool of molten metal. The probe was kept immersed for at least 10-12 seconds and for the time its response became sufficiently stable.

At this stage the evacuation of the mould chamber was stopped and the inert gas mixture was introduced into the chamber till it was filled up completely with the gases. The power was next turned on, the molten metal was again heated up for around 2 to 3 minuits before being finally poured into the mould.

Next the top rubber plug was then removed and the furnace was tilted and a small amount of metal was poured into the copper mould. After the copper mould was almost filled up, it was withdrawn and the furnace was tilted progressively till almost all metal was poured into the mould. As soon as pouring was over, the furnace was brought back to its original position

and suction sampling was done again from the mould. The power was then put off however the cooling water circulation was kept open for next 10-12 hours.

The ingot was next allowed to cool in atmosphere for around an hour and then quenched with water. Once the ingot mould attained the room temperature, it was removed out of the mould and taken for further investigation.

CHAPTER III

RESULTS AND DISCUSSIONS

Altogether eleven experiments were conducted in a laboratory induction furnace. These experiments were done under three different conditions,

(i) melting and casting under normal atmosphere,

(ii) melting and casting under nitrogen atmosphere,

and (iii) melting and casting under nitrogen-argon atmosphere.

However because of some unforseen technical troubles, necessary data couldnot be collected in all these eleven experiments. Some of the problems are presented in table III.1., together with the experimental conditions. Of these eleven experiments, eight were considered satisfactory and were selected for further investigations. In a nut-shell the procedures followed in each experiment is reiterated below :

(i) temperature measurement of the steel bath by thermocouple,

(ii) deoxidiser additions,

(iii) suction sampling from the melt for determination of total oxygen content as well as nitrogen in steel,

(iv) oxygen probe immersion into the melt,

(v) melt sampling in copper mould for C, Si and Mn determination,

T A B L E   III.1

EXPERIMENTAL CONDITIONS AND REMARKS

EXP. No.	DATE OF EXP.	ATMOSPHERE FOR MELTING AND CASTING	MELT TE-MP., °C	DESIRED MELT COMPOSITION						REMARKS
				%O	%Si	%Mn	%C	%N	H (ppm)	
1.	1.7.81	AIR	1657	0.015	0.10	0.60	0.15	0.011	2	
2.	8.8.81	NITROGEN	—	0.020	0.183	0.994	0.15	0.011	4	Oxygen probe didnot function.Hence not considered for investigation.
3.	7.11.81	NITROGEN	1520	0.0170	0.266	1.03	0.15	0.011	4	
4.	14.11.81	NITROGEN+ARGON	1537	0.0180	0.232	1.03	0.15	0.01	4	
5.	15.12.81	NITROGEN+ARGON	1565	0.0370	0.057	0.413	0.15	0.01	4	
6.	17.12.81	NITROGEN+ARGON	1582	0.0180	0.092	0.617	0.15	0.01	4	
7.	18.12.81	NITROGEN+ARGON	1582	0.023	0.10	0.643	0.4	0.01	4	Ingot was not obtained due to bad pouring.Hence not considered.
8.	9.1.82	NITROGEN+ARGON	1504	0.008	0.157	0.814	0.10	0.01	4	
9.	11.1.82	NITROGEN+ARGON	1591	0.007	0.263	1.03	0.15	0.01	4	
10.	15.1.82	NITROGEN+ARGON	1559	0.010	0.101	0.821	0.15	0.01	4	Oxygen probe did not function.Hence not considered.
11.	18.1.82	NITROGEN +ARGON	1590	0.010	0.056	1.02	0.15	0.01	4	Oxygen probe did not function.Hence not considered.

(vi)   pouring molten metal into the mould,

(vii)   occasional suction sampling from the mould
        for oxygen determination,

(viii) ingot slicing,

(ix)   SEM and EPMA of inclusions from the region
        of 90 pct. solidification,

(x)   chemical and spectroscopic analysis of the
        copper mould sample,

(xi)   analysis of oxygen and nitrogen by inert
        gas fusion apparatus.

Of these, ingot slicing, macro and microexaminations
of ingots were carried out by D.R. Kulkarni and are reported
elsewhere[18]. Table III.2 summarises all the experimental find-
ings.

III.1   ANALYSIS,SAMPLING AND MEASUREMENTS

III.1.1   Comparison of bath chemical analysis by spectrosc-
          opic and wet chemical method

The total gas pressure (P_T) at 90 pct. solidifica-
tion is to be calculated from the composition of the steel
melt. Therefore any error in the chemical analysis would in-
troduce deviation from the actual value of P_T. Analysis of
Mn and Si were carried out by wet chemical method. Carbon was
determined by combustion method. Again some of these samples
were analysed for all these elements by spectroscopy as cross
check.

T A B L E   III.2

EXPERIMENTAL FINDINGS

EXPT NO.	ACTUAL COMPOSITION OF THE MELT						AVERAGE TOTAL OXYGEN CONT. OF THE MELT, WT %	CALC-ULAT-ED P_T (90) atm.	AVERA-GE TO-TAL OXYGEN CONT. OF THE INGOT, WT %	EQUL. OXYGEN CONT. OF THE MELT WT %
	% O	% Si	% Mn	% C	% N	H ppm				
1.	0.0441	0.02	0.24	0.06	0.0084	2.5	0.0391	1.67	0.1426	0.0652
3.	0.0032	0.20	1.05	0.17	0.018	2.5	0.0075	0.895	–	0.0053
4.	0.0062	0.23	0.76	0.18	0.0095	2.5	0.0131	0.87	–	0.0075
5.	0.0480	0.01	0.10	0.10	0.0065	2.5	0.0195	1.56	0.0706	0.0545
6.	0.0520	0.01	0.30	0.06	0.0042	2.5	0.0434	0.90	0.0133	0.0382
8.	0.0026	0.15	1.0	0.20	0.0079	2.5	0.0069	0.54	0.0718	0.0051
9.	0.0053	0.03	0.72	0.20	0.0060	2.5	0.0146	0.81	–	0.0215
11.	0.0092	0.07	0.60	0.14	0.0034	2.5	0.0212	0.721	–	0.0178

Table III.3 presents the result of chemical analysis obtained by the above two methods. This shows that the deviation is significant in all the cases for manganese (20 to 30 pct.). However carbon and silicon contents reported by the two methods are within reasonable agreement. In general, the spectroscopic method tends to give higher values. For low silicon, spectroscopic method is more reliable. Since some of the copper mould samples obtained were porous, spectroscopic analysis couldnot be performed upon them, and hence the compositions reported by the wet chemical method were considered for the subsequent calculation of gas pressures.

III.1.2   Performance of oxygen probes.

In each experiment one oxygen probe was immersed into the molten steel bath. The oxygen probe which records the temperature and the dissolved oxygen content of the bath simultaneously, was connected to a voltage-time recorder through shielded wires. However as one of the two pens of the recorder went wrong during the course of experiments, the temperature terminals of the probe were connected to a digital milivoltmeter through compensating lead wires. Once steady e.m.f. was obtained, the probe was taken out. During immersion of oxygen probes, the power to the furnace was cut off to avoid any electromagnetic interference. Figure(III.1) shows a trace of the cell e.m.f. as a function of time. This was obtained in experiment 5 and is a typical one obtained in almost all immersions. The trace corresponds well with that

59
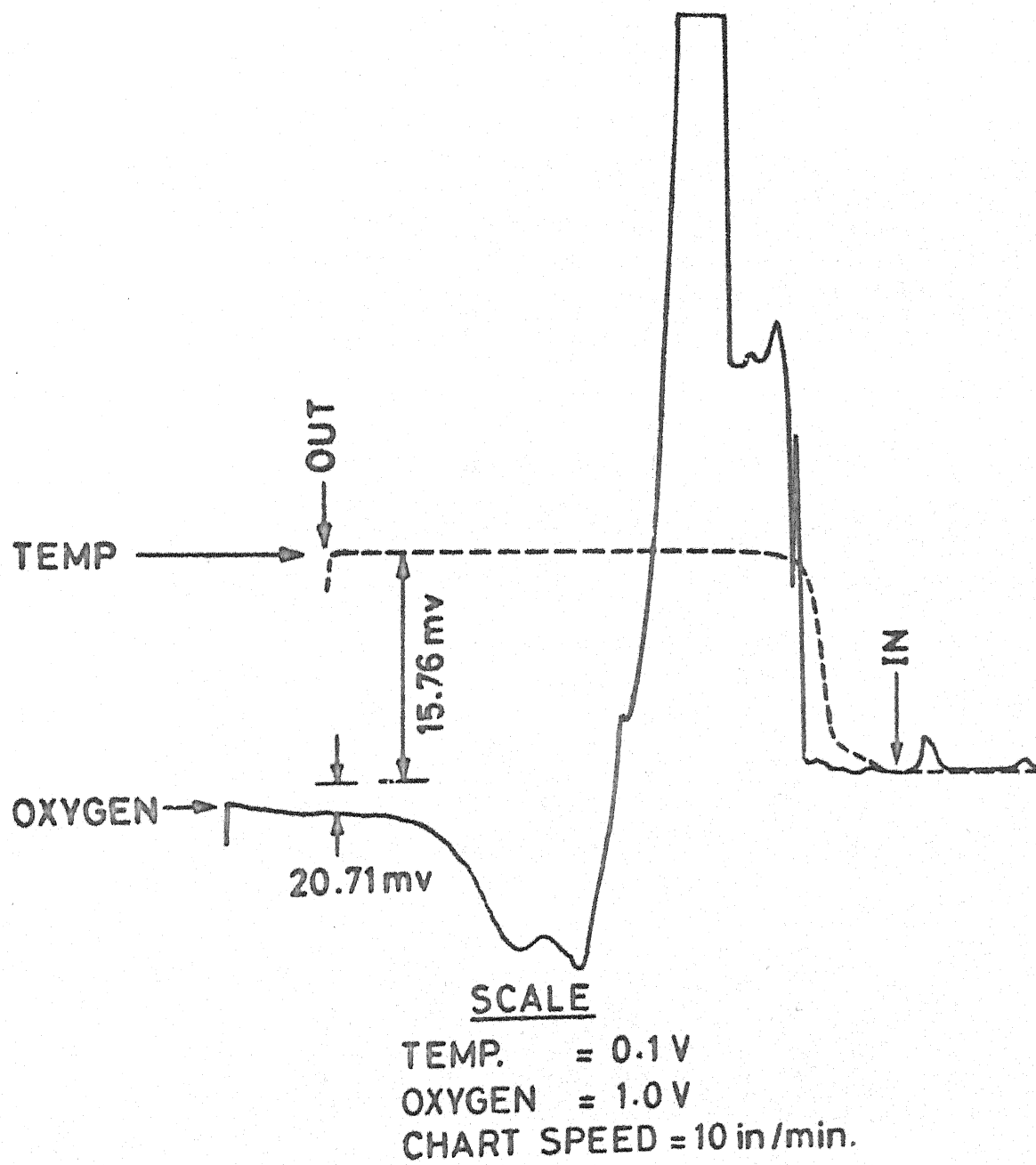
FIG.III.1 TYPICAL PERFORMANCE CURVE
OF OXYGEN PROBE

T A B L E   III.3

BATH CHEMICAL ANALYSIS BY WET CHEMICAL AND
BY SPECTROSCOPIC METHOD

EXPERIMENT NO.	BATH CHEMICAL ANALYSIS					
	WET. CHEMICAL METHOD			SPECTROSCOPIC METHOD		
	%C	%Si	%Mn	%C	%Si	%Mn
1.	0.06	0.02	0.24	–	–	–
3.	0.17	0.20	1.05	0.20	0.22	1.33
4.	0.18	0.23	0.76	–	–	–
5.	0.10	0.01	0.10	–	–	–
6.	0.06	0.01	0.30	–	–	–
8.	0.20	0.15	1.00	0.22	0.16	1.36
9.	0.20	0.03	0.72	0.25	0.07	0.94
11.	0.14	0.07	0.60	–	–	–

reported in literature[19]. The activity of oxygen $[h_0]$ was calculated from the e.m.f. and temperature using equation (2.1). From $[h_0]$, wt.pct. oxygen dissolved in molten steel was calculated using the equation,

$$\log[wt \% \ O] + e_0^C [wt \% \ C] + e_0^{Mn}[wt \% \ Mn] + e_0^{Si}[wt \% \ Si] + e_0^O [wt \% \ O] = \log [h_0] \quad \ldots \ldots \ (3.1)$$

The various interaction parameters are reported in table III.8.

Table III.4 summarises the performance of oxygen probes in all the experiments. It may be noted that the time to attain steady state e.m.f. ranged between 5 to 30 seconds.

III.1.3   Reliability of determination of total oxygen content in steel.

As discussed in chapter II, suction samples were taken from steel melts for determaination of total oxygen content. From each sample button, duplicate samples were prepared for analysis by LECO oxygen determinator. These revealed that besides one or two intances, the values of duplicate samples differed markedly. Comparisons are shown in table III.5. At this stage it may be reiterated that during the initial stages of the investigation, samples were taken in tubes containing air, however at the later stages, it was practised in tubes filled with nitrogen and argon. Review of the results from table III.5 shows that :

(i)   not much improvement in reproducibility was obtained when air tube sampling was replaced by inert gas tube sampling,

T A B L E   III.4

PERFORMANCE   OF   IMMERSION   OXYGEN   PROBES

EXPERI-MENT NO.	TEMP, $^{\circ}$C	STEADY EMF VALUE (mv)	[h_O]	[wt % O]	TIME TO REACH STEADY VALUE, SEC.
1.	1657	150	0.0399	0.0441	9
2.	1520	20	0.0024	0.0032	20
4.	1537	50	0.0045	0.0062	25
5.	1565	206	0.0423	0.0480	21
6.	1580	175	0.0471	0.0520	21
8.	1582	230	0.0021	0.0026	21
9.	1504	20	0.0041	0.0053	25
11.	1559	67	0.0076	0.0092	30

T A B L E   III.5

TOTAL OXYGEN AND DISSOLVED OXYGEN CONTENT
OF THE MELT

EXPERIM-ENT NO.	TOTAL OXYGEN CONTENT OF THE MELT IN DUPLICATE SUCTION SAMPLES, [wt %]	DISSOLVED OXYGEN CONTENT OF THE MELT, [wt %]
1.	0.0322, 0.0461	0.0441
3.	0.0047, 0.0103	0.0032
4.	(0.0118),(0.0144)	0.0062
5.	(0.0195),	0.0480
6.	(0.0438),(0.0430)	0.0520
8.	(0.0069),	0.0026
9.	(0.0130),(0.0162)	0.0053
11.	(0.0247),(0.0177)	0.0092

( ) stands for samples obtained by inert gas tubes and the
unbracketed figures stand for samples obtained by air tubes.

and   (ii)   the total oxygen content of the melt, as
              expected is higher than the dissolved oxy-
              gen content. This shows that the contribu-
              tion of oxygen in the inclusions was more
              significant than dissolved oxygen alone.

The issue of irreproducibility as well as the ab-
ove observations received our attention during the course
of the investigation and it was then decided to conduct add-
itional experiments, so that factors contributing to these
could be explained with reasonable arguments. Detailed anal-
ysis of the problem revealed that there might be two possible
reasons contributing to the differences. These were identifi-
ed as :

              (i)   uneven and irreproducible distribution of
                     inclusions in samples,

and   (ii)   likely absence of some amount of undissolved
              aluminium in the sample buttons.

To throw more light on these, the following data
collection programme was undertaken during the additional
experiment :

              (i)   the distribution of inclusions in the molten
                     steel bath is expected to change with time
                     after the addition of deoxidisers because of
                     the fact that floatation of inclusions is a
                     slow process. Also under such a condition, if
                     sampling is done at several time intervals, a
                     characteristic time which corresponds to a
                     stage when most of the inclusions are floated

up can be determined. It is expected that as more and more of the inclusions float, the distribution pattern of inclusions in the suction samples can no longer contribute to the deviation pointed out earlier,

(ii) quantity of aluminium wires should be more than sufficient. Stoichiometric calculations show that around 100 mg of aluminium wire is more than adequete for 10 gram samples. Also the cross-sections of the steel samples should be observed to ensure that there was significant amount of undissolved aluminium left,

(iii) three samples were to be prepared for analysis from the same button. This was to check on existence of oxygen gradient along the length of a button, if any,

and (iv) sampling was to be done with both air and inert gas filled tubes.

Around 6 Kg. of mild steel rounds were melted in the induction furnace. After the addition of deoxidisers (ferromanganese and ferrosilicon) suction samples were taken at different interval of time by the above two methods. Standardsized samples were prepared from the buttons, which were subsequently cleaned and visually inspected. The results of oxygen determination on these samples are presented in table III.6.

The table reveals that the total oxygen content of the steel melt diminishes with time, which confirms about the float-

T A B L E   III.6

ANALYSIS   OF   VARIATION   OF   OXYGEN
CONTENT   IN   SUCTION   SAMPLES

SERIAL NUMBER	TIME AFTER ADDITION OF DEOXIDISERS AT WHICH SAMPLE WAS TAKEN, (min.)	OXYGEN CONTENT OF THE BUTTON, wt %			AVERAGE OXYGEN CONTENT OF THE BUTTON, wt %
		FRONT END	MIDDLE	BACK END	
1.	5	0.0197 (-)	0.0228 (-)	0.0134 (-)	0.0186 (-)
2.	8	0.0104 (0.0117)	0.0165 (0.0091)	0.0098 (0.0075)	0.0123 (0.0094)
3.	11	0.0112 (-)	0.0089 (0.0087)	0.0114 (0.0068)	0.0105 (0.0077)
4.	35	0.0083 (0.0107)	0.0115 (0.0140)	0.0119 (0.0132)	0.0106 (0.0126)

(   ) stands for samples obtained by inert gas tubes whereas

the unbracketed figures stand for samples obtained by air

tubes.

ation of inclusions with time. Under this situation, if oxygen probe is immersed immediately after the addition of the deoxidisers the correspondence between dissolved oxygen and total oxygen values are expected to be poor. Hence the disagreement between the two as presented in table III.5 may be accounted for this reason . Thus it can be concluded from the trends of variation of oxygen content in suction samples that, if the suction sample is taken from the melt about 10 min. after the addition of deoxidisers, the dissolved as well as total oxygen contents are likely to be close.

Regarding the comparative performance of inert gas tube and air tube sampler, nothing can be conclusively stated, though the average oxygen content obtained by the inert gas tube for the initial period were lower than the corresponding values obtained by the air tube. However, the sudden shooting up of oxygen content towards the end as shown in table III.6 is surprising.

Furthermore, the table III.6 reveals that there exists significant variation of oxygen content in the samples taken from the same button. Thus to obtain a representative value of the melt oxygen content, atleast three samples are to be analysed from the same button, so that a reasonable average value can be obtained.

III.2   ESTIMATION OF HYDROGENT CONTENT OF MELT AFTER
         TEEMING FROM THEORETICAL CONSIDERATIONS

Hydrogen determination, like oxygen determination, or nitrogen determination was not performed on melt suction samples. Since the diffusivity of hydrogen is quite high, the samples after they were being taken from the melt, required to be stored at subzero temperature. This can be facilitated by either storing them in solid ice or in liquid nitrogen. However, as a hydrogen determinator was not available within reach, this further required transporation of the samples at subzero temperature to a place, where such an equipment was readily available. Owing to this, it was thought of at the earlier stage of the investigation that a value of hydrogen content of the melt is to be estimated by considering the thermodynamics and kinetics of hydrogen absorption in molten steel.

So far as the thermodynamic calculations are concerned, hydrogen in steel may be assumed to attain equilibrium,

      (i)   with respect to the furnace atmosphere,

and   (ii) with respect to the atmosphere in the open air during melting and casting of steel.

Hydrogen is absorbed from the atmosphere through the reaction,

$$H_2O\ (g) = 2\ [H] + [O] \qquad \ldots\ldots\ (3.2)$$
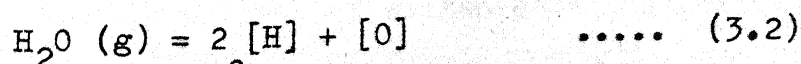
and $$K_3 = \frac{[h_H]^2 \cdot [h_O]}{p_{H_2O}} \qquad \ldots\ldots\ (3.3)$$

where,

K_3 is the equilibrium constant defined by the equation (3.2).

Value of K_3 is reported in table III.9. Values of $[h_O]$ and

temperature are available in table III.3. $[h_H]$ for all exper-

iments could be calculated assuming equilibria with the furn-

ace atmosphere or outside atmosphere. $[h_H]$ was converted into

[wt.pct.H] with the help of the following equation.

$$\log[h_H] = \log[wt \; \% \; H] + e_H^{Si}[wt \; \% \; Si] + e_H^{Mn}[wt \; \% \; Mn] + e_H^{O}[wt \; \% \; O]$$
$$+ e_H^{C}[wt \; \% \; C] + e_H^{H}[wt \; \% \; H] \qquad \ldots\ldots \quad (3.4)$$

The values of e_H^{J} are reported in table III.8.

The p_{H_2O} in the furnace was calculated from the ana-

lysis of the flushing gases as reported by the supplier, while

that in the open atmosphere was calculated from the measured

room temperature and relative humidity. Table III.7 summarises

the equilibrium calculations, (i) with respect to the furnace

p_{H_2O} and (ii) with respect to the p_{H_2O} in the atmosphere. These

calculations show that minimum hydrogen content of the melt was

expected to be 0.2 ppm, whereas the maximum (in equilibrium with

(ii)) was approximately 38 ppm. Since both of these are quite

unlikely, we have to consider the kinetics of hydrogen absorption

to arrive at a reasonable value of hydrogen content of the metal

at the time it enters the mould.

Various investigators have reported the amount of oxy-

gen absorped during teeming of molten steel as follows :

T A B L E   III.7

EQUILIBRIUM HYDROGEN CONTENT OF METAL WITH RESPECT
TO THE p_{H_2O} IN THE FURNACE AND WITH RESPECT TO THE
p_{H_2O} IN THE ATMOSPHERE

EXP. NO.	TEMPER- ATURE, $^\circ C$	ATMOSPHERE p_{H_2O}	FURNACE p_{H_2O}	$[H]_{ppm}$ IN EQUL.WITH ATMOS. p_{H_2O}	$[H]_{ppm}$ IN EQUL.WITH FURNACE p_{H_2O}
1.	1657	0.0415	0.0415	22.7	22.7
3.	1520	0.0219	0.24×10^{-4}	39.96	1.32
4.	1537	0.0169	0.24×10^{-5}	29.17	0.347
5.	1565	0.0142	0.87×10^{-5}	9.74	0.241
6.	1582	0.0124	0.87×10^{-5}	9.1	0.241
8.	1504	0.0157	0.87×10^{-5}	38.99	0.917
9.	1591	0.0169	0.87×10^{-5}	35.23	0.799
11.	1590	0.0140	0.87×10^{-5}	23.46	0.585

T A B L E   III.8

EQUILIBRIUM CONSTANT VALUES AS A FUNCTION
OF   TEMPERATURE

EQUILIBRIUM CONSTANT	VALUE
$\log K_3$	$-\dfrac{10847.76}{TEMP} + 8.03$
$\log K_{11}$	$-\dfrac{14450}{TEMP} - 6.43$
$\log K_6$	$\dfrac{1510}{TEMP} + 1.27$
$\log K_{16}$	$\dfrac{30410}{TEMP} - 11.59$
$\log K_{17}$	$\dfrac{1168}{TEMP} + 2.07$
$\log K_{19}$	$-\dfrac{1637}{TEMP} - 2.316$
$\log K_{20}$	$-\dfrac{188.1}{TEMP} - 1.246$
$\log K_{13}$	$\dfrac{510}{TEMP} + 1.77$
$\log K_{12}$	$\dfrac{14950}{TEMP} - 6.68$

T A B L E   III.9

INTERACTION PARAMETER VALUES USED IN THE PRESENT INVESTIGATION

SOLUTE - J	e_C^J	e_O^J	e_H^J	e_N^J	e_{Si}^J	e_{Mn}^J
C	0.22	-0.41	0.06	0.130	$\frac{380}{TEMP}$ -0.023	- 0.07
O	- 0.31	-0.20	-	-	- 0.23	- 0.083
Mn	- 0.012	-0.021	-0.0014	-0.023	0.002	0.0
Si	0.07	-0.016	0.027	0.047	$\frac{34.5}{TEMP}$ +0.089	0.002

TEMPERATURE = $1600^{o}C$

Investigators	Oxygen absorption during teeming, ppm
Larsen and coworkers[20]	1000
Kenny[21]	30
Wilson[22]	9
Kurita[23]	5
and Samways[24]	100-200

On the basis of oxygen determination of the mould suction samples outlined in section III.4.1, together with the previous informations on factors governing absorption of gases from atmosphere during teeming, we make an assumption that around 400 ppm of oxygen could be absorbed during taming in this investigation, if the stream were to fall through the atmosphere. Since N_2 - Ar mixture was flushed continuously through the mould chamber, we can assume that at any stage the gas envelope sorrounding the stream was around 50 pct. air and 50 pct. N_2 - Ar mixture. Under such a condition, the amount of oxygen absorbed could be somewhere around 200 ppm.

Since oxygen may be absorbed (i) from oxygen in atmosphere and from (ii) H_2O in atmosphere, and since average moisture content of atmosphere was around 2 pct., as compared to 20 pct. oxygen in air. We can roughly say that $\frac{1}{20}$ th of the total oxygen comes from H_2O in the atmosphere, whereas the rest from the atmospheric oxygen. Under such a condition the amount of oxygen absorbed from atmospheric moisture is 200/20 i.e. 10 ppm. Since in a molecule of H_2O, there are 2:16 parts of hydrogen:oxygen, the corresponding amount of hydrogen absorbed is $\frac{10}{8}$ i.e. 1.25 ppm.

The initial hydrogen content of molten steel before pouring in equilibrium with the furnace atmosphere is on the average 0.5 ppm. Recognizing that there will be some leakage of air in the furnace atmosphere, this value may be around 1 ppm or so. Therefore the total hydrogen content of the steel is expected to be above 2 ppm after pouring.

Harkness et al[11] have reported of hydrogen pick up from the atmosphere to the extent of 2 ppm. Hence it is quite reasonable for us to conclude that about 2.5 ppm in the cast ingot upon teeming is most likely.

III.3   THERMODYNAMIC CALCULATIONS AND THEIR INTERPRETATIONS

III.3.1   Dissolved oxygen content of the melt and its relationship with Si-Mn-O equilibrium:

Whether or not the values of dissolved oxygen correspond to those predicted by equilibrium, can be determined by duly considering the silico-manganese deoxidation reaction which is represented below. The calculations were performed in computer. The programme is a modified version of the one developed by Bagaria[13].

$$Si[wt \%] + 2MnO(s) = 2Mn[wt \%] + SiO_2(s) \quad \dots (3.5)$$
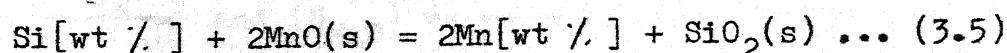
$$\text{and} \quad K_b = \frac{(a_{SiO_2})}{(a_{MnO})^2} \cdot \frac{[h_{Mn}]^2}{[h_{Si}]} \quad \dots (3.6)$$

where, K_6 is the equilibrium constant defined by the equation (3.5). The value of K_6 as a function of temperature is given in table III.9.

The equation III.5 can be rewritten as :

$$\frac{(a_{SiO_2})}{(a_{MnO})^2} = K_6 \frac{[h_{Si}]}{[h_{Mn}]^2} \qquad \dots \dots \quad (3.7)$$

The values of h_{Mn} and h_{Si} were calculated from the chemical analysis of the bath (tables III.3 and III.4) and the standard interaction coefficient values (table III.8) by the following equations :

$$\log[h_{Mn}] = \log[wt~\%~Mn] + e_{Mn}^C[wt~\%~C] + e_{Mn}^O[wt~\%~O] + e_{Mn}^{Si}[wt~\%~Si] +$$

$$e_{Mn}^{Mn}[wt~\%~Mn] \qquad \dots \dots \quad (3.8)$$

and $\log[h_{Si}] = \log[wt~\%~Si] + e_{Si}^C[wt~\%~C] + e_{Si}^O[wt~\%~O] + e_{Si}^{Mn}[wt~\%~Mn]$

$$+e_{Si}^{Si}[wt~\%~Si] \qquad \dots \dots \quad (3.9)$$

K_6 was calculated from the knowledge of bath temperature (table III.4) and thus the ratio, $(a_{SiO_2})/(a_{MnO})^2$, were obtained from Eq.(3.7).

The activity of silica (a_{SiO_2}) and manganese oxide (a_{MnO}) as a function of mole fraction of manganese oxide (N_{MnO}) at $1500^\circ C$ and $1650^\circ C$ have been reported by Abraham et al[25]. From these values, relations between (a_{MnO}) vs $\frac{(a_{SiO_2})}{(a_{MnO})^2}$, (a_{SiO_2}) vs $\frac{a_{SiO_2}}{(a_{MnO})^2}$ and (N_{MnO}) vs $\frac{a_{SiO_2}}{(a_{MnO})^2}$ were obtained by least square method. For intermediate temperatures between $1500^\circ C$ and $1650^\circ C$, interpolations were done to calculate (a_{SiO_2}) and (a_{MnO}) corresponding to a particular (N_{MnO}). The interpolated values were subsequently used for the least square method.

For the particular values of $\dfrac{(a_{SiO_2})}{(a_{MnO})^2}$, obtained elarlier from $[h_{Si}]$ and $[h_{Mn}]$ vide equation (3.7), the corresponding values of (a_{SiO_2}), (a_{MnO}) and (N_{MnO}) were calculated. Once (a_{MnO}) was obtained, the following equation was used to obtain the activity of oxygen $[h_O]$

$$Mn[wt \%] + O[wt \%] = MnO \ (s) \quad \ldots \ldots \quad (3.10)$$
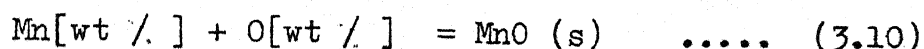
$$K_{11} = \frac{(a_{MnO})}{[h_{Mn}][h_O]} \quad \ldots \ldots \quad (3.11)$$

where K_{11} is the equilibrium constant defined by the equation (3.10). The value of K_{11} as a function of temperature is presented in table III.9.

After $[h_O]$ was calculated from equation (3.11), $[wt \% O]$ was calculated by a trial an error method from equation (3.1).

Table III.10 presents the value of equilibrium · oxygen content of the bath along with the experimentally determined the dissolved oxygen content of the same. The results were subsequently compared with those reported by Bagaria[13], and reasonable agreement was obtained.

It shows that there exists three different types of situations, viz.,

(i) the dissolved oxygen content is higher than the calculated equilibrium oxygen content, [Exp.No. 6]

(ii) the dissolved oxygen content is approximately equal to the equilibrium oxygen content, [Exp. No. 4]

T A B L E   III.10

DISSOLVED OXYGEN CONTENT AND CALCULATED EQUILIBRIUM

OXYGEN   CONTENT   OF   THE   MELT

EXP.NO.	DISSOLVED OXYGEN CONTENT OF THE BATH, WT /	CALCULATED EQUILIBRIUM OXYGEN CONTENT OF THE BATH		EQUILIBRIUM SLAG COMPOSITION	
		$[h_O]_{EQ}$	$[WT / O]_{EQ}$	N_{MnO}	a_{MnO}
1.	0.0441	0.059	0.0652	0.50	0.17
3.	0.0032	0.004	0.0053	0.50	0.219
4.	0.0062	0.006	0.0075	0.49	0.173
5.	0.0480	0.047	0.0545	0.45	0.130
6.	0.0520	0.034	0.0382	0.51	0.234
8.	0.0026	0.004	0.0051	0.51	0.233
9.	0.0053	0.017	0.0215	0.56	0.281
11.	0.0092	0.0150	0.0178	0.51	0.203

and   (iii) the dissolved oxygen content is lower than
the equilibrium oxygen content.

[Exp.Nos. 1,3,5,7,9 and 11]

Of these, the first two types of situations are
normally encountered during steelmaking operation and is
also reported by Harkness et al[11]. However, the situation
(iii) in which the dissolved oxygen values are lower as
compared to the calculated equilibrium values, is difficult
to understand, because this is unexpected from theory. To
evaluate the possible reasons for this phenomenon,
thermodynamic data from various other sources[26] were
used in order to have more confidence on calculations. This,
however, didnot alter the situation significantly. One of
the probable reasons which can account for this anamoly may
be the presence of considerable oxygen gradient in the molten
steel bath owing to poor mixing of the deoxidisers.

III.3.2   Variation of p_{CO}, p_{H_2}, p_{N_2} and P_{Total} with progress
of solidification:

The chemical compositions of steel melts (oxygen,
carbon, silicon, manganese, hydrogen and nitrogen) were fed
into the computer programme[12] to calculate the gas pressures
with the progress of solidification. It has been pointed out
by Turkdogan (sec. I.2.1) that oxygen in solution is the key
element which reacts with other dissolved solutes during soli-
dification. A few sample results about the trend of variation

of dissolved oxygen in the interdendritic liquid with progressive solidification is presented in table III.11. The table reveals that in some of the cases, oxygen content of the interdendritic liquid first increases and then decreases progressively, while in the rest, the oxygen content of the interdendritic liquid starts decreasing right from the commencement of solidification. The increase in oxygen content is due to the rejection of oxygen from the solidifying metal into the liquid according to the equilibrium partition coefficient K ($= \frac{C_s}{C_l} < 1$). However the decrease is due to the onset of critical stage of deoxidation, i,e, the moment at which Si-Mn-O reaction sets in the interdendritic liquid. The trend is identical in nature to the one reported in literature[8].

Figures III.2 to III.4 present some examples of the trends in the variation of P_{CO}, P_{N_2}, P_{H_2} and P_{Total} with the progress of solidification. In general it is expected that P_{CO} will first increase with the progress of solidification and then decrease especialy towards the latter stage of solidification due to the deoxidation reaction. It may be noted that P_{CO} depends upon the value of the product [wt % C]x[wt % O] in the interdendritic liquid at any stage of solidification. If [wt % C]x[wt % O] tends to decrease, P_{CO} accordingly decreases. However if [wt % C]x[wt % O] tends to increase, P_{CO} increases. Oxygen and carbon in solution in molten steel increase due to segregation while both of them decrease due to a shift in transformation from (L $\longrightarrow$ δ_{Fe}) to (L $\longrightarrow$ γ_{Fe}). The natures of

T A B L E   III.11

OXYGEN   ENRICHMENT   WITH   PROGRESSIVE   SOLIDIFICATION

| EXPERI-MENT NO.	WT / OXYGEN AT VARIOUS STAGES OF SOLIDIFICATION						GENERAL COMMENTS
	0 %	20 %	40 %	60 %	80 %	100 %	
3.	0.0032	−	0.0040	0.0033	0.0025	0.0013	Slight increment and then progressive decrement
6.	0.052 ·	0.0167	0.0150	0.0129	0.0101	0.0062	Progressive decrement
8.	0.0026	−	0.0041	0.0035	0.0026	0.0015	Slight increment and then progressive decrement
9.	0.0053	−	0.0075	0.0063	0.0047	0.0031	Slight increment and then progressive decrement
11.	0.0092	0.0075	0.0067	0.0058	0.0042	0.0032	Progressive decrement
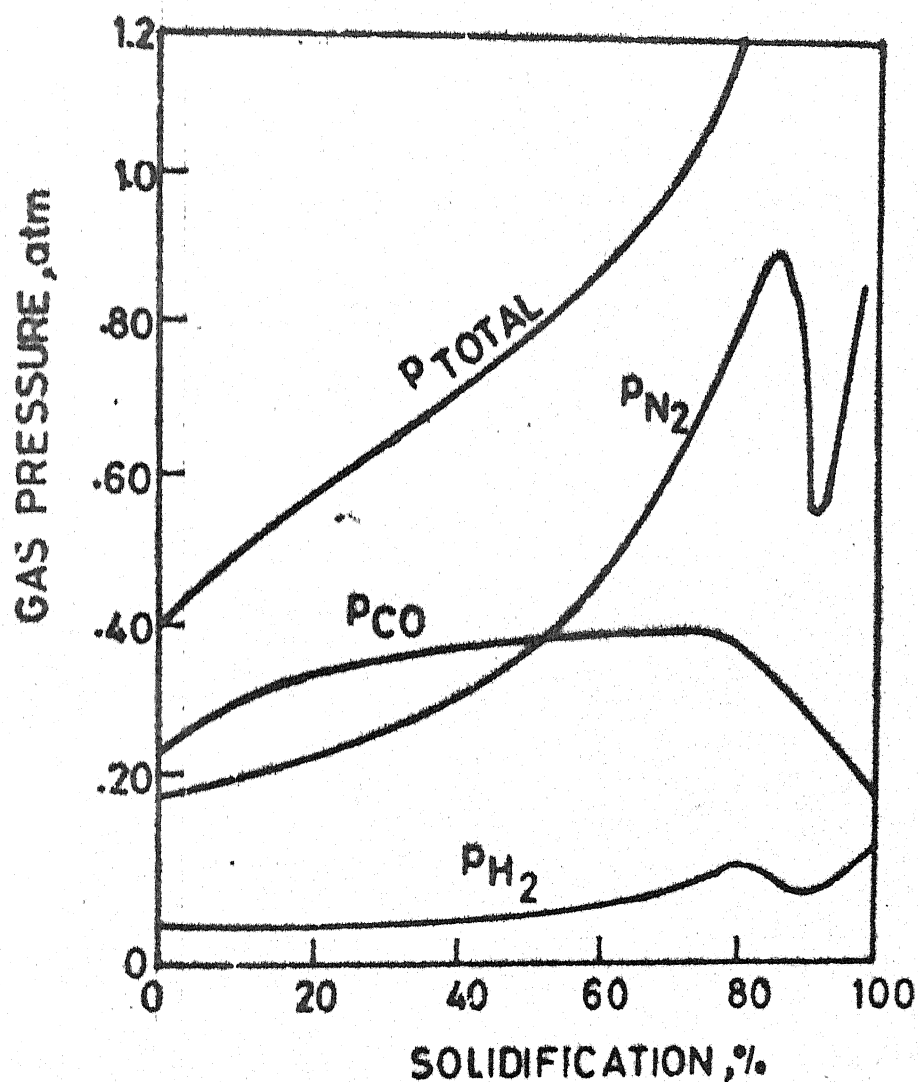
FIG. III.2 VARIATION OF P_{CO} P_{N_2} P_{H_2} AND P_{TOTAL} WITH PROGRESSIVE SOLIDIFICATION (Exp. No. 4)
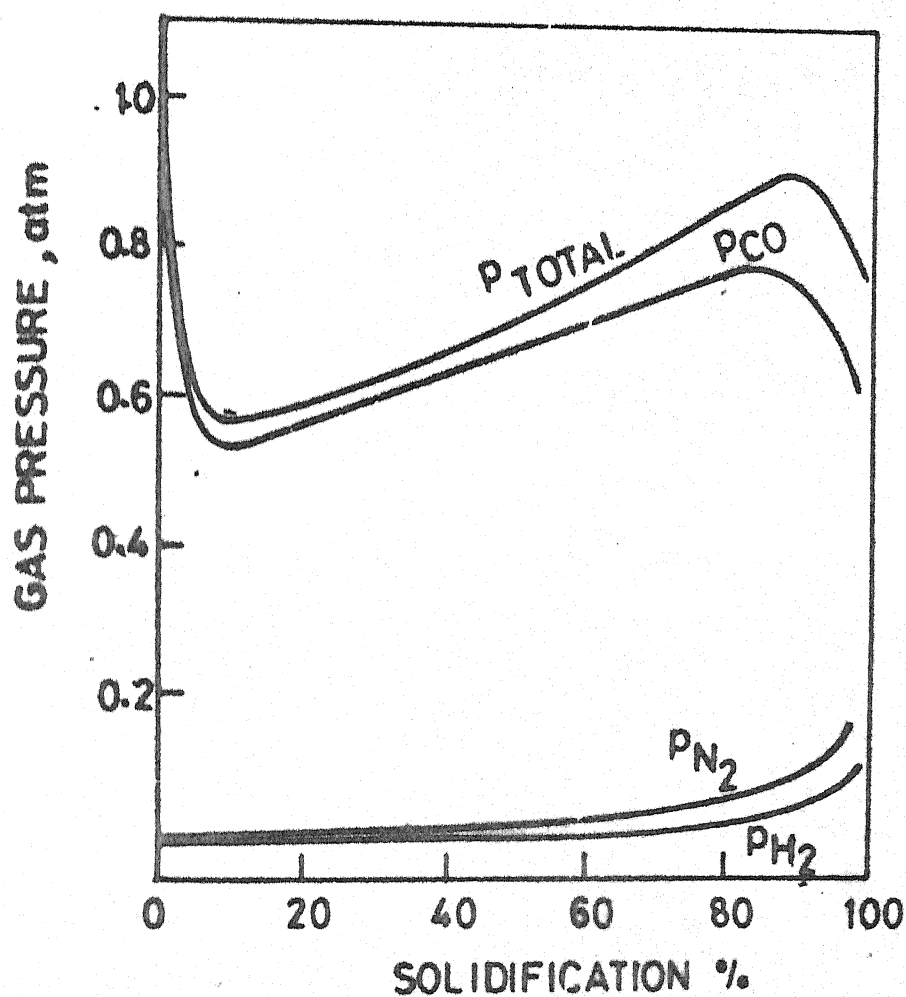
FIG. III.3 VARIATION OF P_{CO}, P_{N_2}, P_{H_2} AND P_{TOTAL} WIDTH PROGRESSIVE SOLIDIFICATION (Exp No. 6)
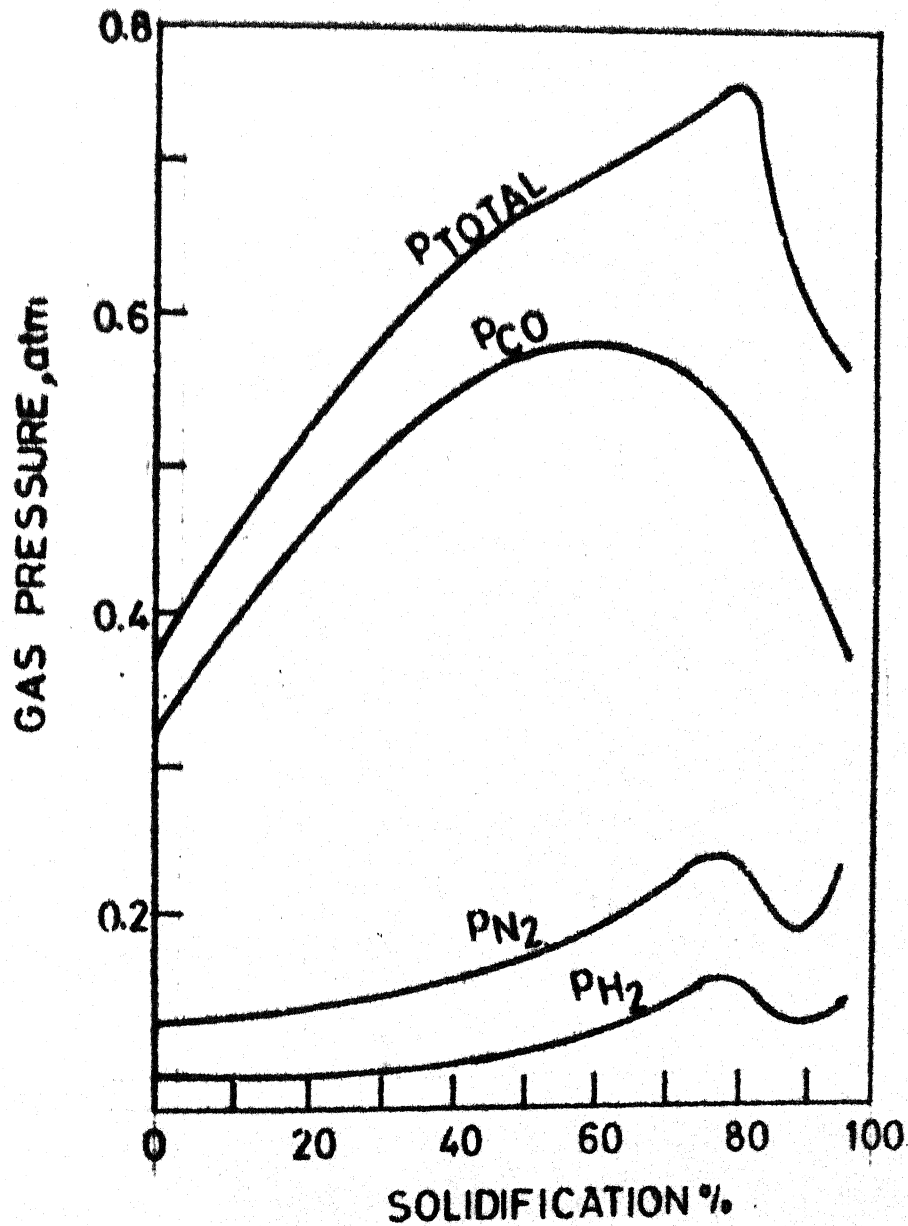
FIG. III. 4 VARIATION OF P_{CO} P_{N_2} P_{H_2} AND P_{TOTAL} WITH PROGRESSIVE SOLIDIFICATION (Exp. No 8)

variation of p_{CO} with progress of solidification, as presented in figures III.2 to III.4, can be explained from the combined effect of all these phenomena on [wt % C]x[wt % O]. For example in fig.III.3, p_{CO} shows a marked decrease initially. This is due to high value of original oxygen content. This led to significant deoxidation by Si+Mn from the very beginning and hence marked decrease in [wt % O] from 520 ppm to 167 ppm (table III.11). Although segregation of carbon simultaneously increased [wt % C] in steel but that effect was much less significant as compared to decrease of [wt % O].

So far the variation of p_{H_2} and p_{N_2} are concerned, the general trend should be identical to one shown in figure III.3. However, the decrease of p_{H_2} and p_{N_2} towards the latter stage of solidification, as have been shown in figures III.2 and III.4, were due to a shift of transformation from $(L \longrightarrow \delta_{Fe})$ to $(L \longrightarrow \gamma_{Fe})$. This shift of transformation occurs when carbon concentration in the interdendritic liquid exceeds the critical value for δ to γ transformation (i.e., 0.5 pct.). Since the equilibrium distribution coefficient of nitrogen, hydrogen and carbon are higher in γ iron than in δ iron, their concentration in the interdendritic liquid is thus expected to decrease. Such decrease in the concentration of hydrogen and nitrogen caused a corresponding decrease in the p_{H_2} and p_{N_2} values, which have been reflected in figures III.2 and III.4.

Thus it becomes clear that if the molten steel solidifies to δ iron (till carbon concentration in solution is less than 0.5 pct.) there will be continuous increase of [wt % H] and [wt % N], in the solution and consequently p_{H_2} and p_{N_2} will also increase. However the moment the molten steel starts solidifying to γ iron (i.e. when carbon in solution exceeds 0.5 pct.), [wt % H] and [wt % N] in remaining melt start decreasing and as a consequence p_{H_2} and p_{N_2} also decrease.

III.4   INTERPRETATION OF INGOT STRUCTURES

III.4.1   Prediction of ingot structures from the total gas pressure (P_T) value at 90 pct. solidification and their agreement with actual ingot structures obtained.

As has been pointed out in section I.2.1, Harkness et al[11] came to the conclusion that ingots become dense when P_{Total} at 90 pct. solidification falls below 1 atm., marginally porous when P_{Total} lies between 1-1.4 atm., and porous when P_{Total} exceeds 1.4 atm. Based upon this criterion, an attempt has been made to predict the ingot structure from the P_{Total} values corresponding to 90 pct. solidification. Table III.12 presents calculated P_T at 90 pct. solidification. It also contains brief comments about the nature of ingots. It should be pointed out here that spectroscopic analysis in general gives higher values of C, Si and Mn (table III.3) as

compared to the wet chemical method. Therefore if these calculations are performed on the basis of spectroscopic analysis the value of P_T will be somewhat lower.

The actual ingot structures were determined by sectioning the ingots vertically, observation of ingot surface under low magnification and blowhole volume measurement[18]. Table III.12 reveals that the agreement between the theoretically predicted ingot structure and actual ingot structure is good with ingots for experiment nos. 1,5,8,9 and 11, whereas the agreement is poor for the rest. Table III.12 however reveals a general feature that there exist a definite tendency for the ingots to become more porous than what is expected from theory.

Figures III.5 to III.7 show some sample macrophotographs of cast ingots[18]. For example, ingot no.8, represented by figure III.7, shows that though otherwise dense, it has one or two blowholes at the top portion. Since the ingot corresponds to a total pressure P_T at 90 pct. solidification around 0.54 atm. blowholes are not expected at all in its cast structure and thus the ingot is expected to be more dense than it actually is. Such a deviation may account for the oxygen absorbed during teeming as discussed below.

Appreciable amount of oxygen absorbed during teeming increases the oxygen content of the metal in the ingot mould and thus, the tendency of the ingots become more porous than expected. It may be noted from table III.12 that the ingots

T A B L E   III.12

THEORETICALLY PREDICTED INGOT STRUCTURE FROM P_T (90 pct)
VALUE AND ACTUAL INGOT STRUCTURE

EXPT. NO.	$P_T (90 \%)$ atm.	STRUCTURE OF THE INGOTS	
		THEORITICAL	ACTUAL
1.	1.67	Porous	POROUS ingot. Blow holes are deep and distributed all over.
3.	.895	Dense	POROUS ingot. Blowholes distributed all over ingot. Rising top.
4.	.87	Dense	POROUS ingot. Blowholes are large and deep.
5.	1.56	Porous	The ingot is very POROUS. Blowholes distributed all over the ingot.
6.	.90	Dense	POROUS ingot. Blowholes all over the ingot.
8.	.54	Dense	Dense ingot.One or two blowholes only in the top part. Almost flat top.
9.	.81	Dense	POROUS/DENSE ingot. Blowholes not deep and big. Flat top.
11.	.72	Dense	POROUS/DENSE ingot. Only a few blowholes in the centre.

FIG.III.5 MACROPHOTOGRAPH OF INGOT(EXP.NO.3)
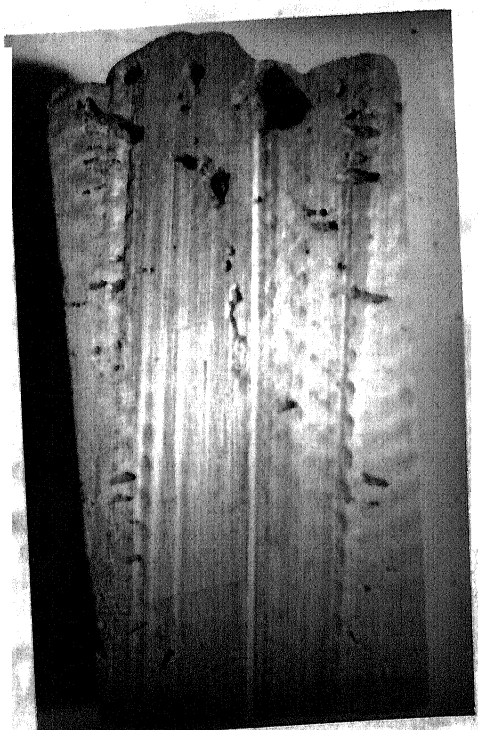
FIG.III.6. MACROPHOTOGRAPH OF INGOT(EXP.NO.11)

FIG.III.7 MACROPHOTOGRAPH OF INGOT(EXP.NO.8)

for which agreement is poor, have P_T values in the range of 0.87 to 0.90 atm. at 90 pct. solidification. Since P_T is close to one atmosphere in the above cases, absorption of oxygen upon teeming would considerably increase their gas content and with the result the ingots becoming porous is not very unlikely.

Occasional suction sampling was practised to obtain samples from the mould for total oxygen determination. However, samples couldnot be taken from some of the moulds because of fast chilling of molten metal in the mould. Nevertheless, the sample upon analysis show that there was considerable absorption of oxygen from atmosphere during teeming. The extent of oxygen absorption during may be visualised from table III.2.

Table III.12 reveals that oxygen absorption is drastically reduced during melting and casting under inert atmosphere as compared to melting and casting under normal atmosphere.

It is to be mentioned here that the suction samples obtained from the mould cannot be a representative one for the entire ingot because of segregation effects. Since the samples were taken at a stage when some metal had already solidified, they corresponded to the enriched oxygen content rather than the average oxygen content of the ingots. To ascertain this three samples were taken from different regions of one ingot.

This is presented in figure III.8. This shows that there is considerable segregation of oxygen in the ingot and the average total oxygen content of the ingot was around 1092 ppm (lower than the value obtained from oxygen determination of mould-suction samples). However this didnot alter the conclusion that significant amount of oxygen was absorbed during teeming.
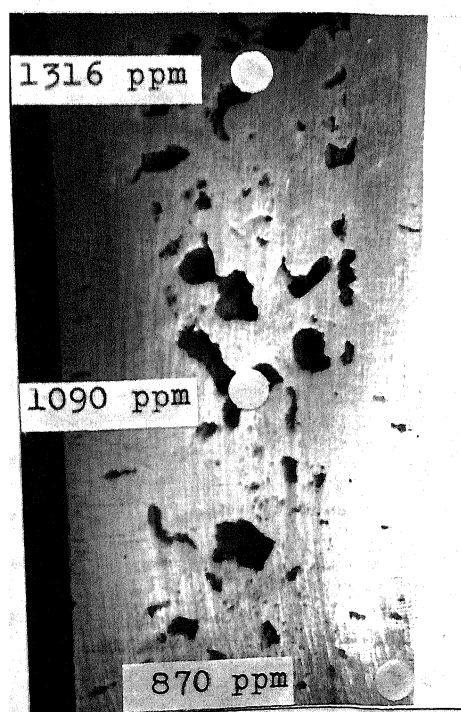
FIG.III.8 SEGREGATION OF OXYGEN IN AN INGOT(EXP.NO.1)

CHAPTER IV

SUMMARY AND CONCLUSIONS

(1) Eleven experiments with molten steel were conducted in a 8 Kg. laboratory induction furnace, of which eight most reliable experiments were selected for further analysis and investigations. These experiments were carried out under three different conditions viz., melting and casting under air, melting and casting under nitrogen and melting and casting under nitrogen-argon mixture. Controlled deoxidations were carried as per program already chalked out.

(2) Samples were collected from the furnace bath (a) after the addition of deoxidisers and (b) just before tapping for analysis of total oxygen content by inert gas fusion apparatus as well as for analysis of elements C,Mn and Si. Occassionally, samples were also taken from the mould for total oxygen determination.

(3) Dissolved oxygen content of the melt after the addition of deoxidisers was measured by immersion oxygen probes.

(4) The molten metal was poured in the mould. The ingots thus produced were subsequently sectioned vertically. Macroscopic and microscopic examinations were carried out upon them by D.R. Kulkarni[18].

(5) Chemical composition of the bath determined by spectroscopic method tended to give higher values over conventional wet chemical method.

(6) The total oxygen content of the melt, as expected, was higher than the dissolved oxygen content. This shows that the contribution of oxygen in the inclusions to total oxygen values was as significant as that of oxygen dissolved in molten steel.

(7) The dissolved oxygen content as well as the total oxygen content is likely to be close, if the suction sample is taken from the melt about 10 min. after the addition of deoxidisers.

(8) To obtain a representative value of the total oxygen content in steel atleast three samples are to be analysed from the same sample button, so that a reasonable average value can be obtained.

(9) Total oxygen content of the ingot was appreciably higher than that of the melt. However the deviation between the two was considerably reduced when casting were done under controlled condition (nitrogen-argon atmosphere) than under air.

(10) Thermodynamically predicted ingot structures are within reasonable agreement with the actual ingot structures, though there exist a definite tendency for the ingots to become more porous than is predicted from theory. This is attributed to the absorption of oxygen from atmosphere during teeming.

(11) Experimentally measured values of dissolved oxygen in molten steel was observed to scatter around the values of the same as calculated thermodynamically for deoxidation by silicon and manganese.

(12) The variation of partial pressures of p_{CO}, p_{H_2} and p_{N_2} with progress of solidification were examined and reasonable agreement with that in literature was established.

CHAPTER   V

RECOMMENDATIONS FOR FURTHER WORK

Inorder to make the experimental findings more worthy, the following improvements upon the existing programme is envisaged.

(1)   Hydrogen content of the metal in the furnace as well as in the mould will have to be determined by inert gas fusion apparatus.

(2)   The investigation will have to be carried out in a vacuum/inert gas induction melting unit.

(3)   The investigation will have to be extended to the largescale production of ingots in the industrial sectors.

REFERENCES

1. K.G. Trubin and G.N. Oiks, Steelmaking - Open Hearth and Combined Processes, Mir Publishers, Moscow (1974).

2. G.R. Bashforth, The Manufacture Of Iron and Steel, Vol.2, Asia Publishing House, Bombay (1960).

3. A. Ghosh, Keynote address in the discussion meeting Making and Processing of Semikilled and Rimming Steel, Rourkela, July (1982).

4. H.N. Dharwarkar, Ph.D. Thesis, Dept. of Met. Engg., I.I.T., Kanpur (1982).

5. R.G. Ward, An Introduction to Physical Chemistry of Iron and Steelmaking, Edward Arnold, U.K. (1962).

6. D. Burns and J. Beech, Ironmaking and Steelmaking, 1 (1974) pp. 364 - 374.

7. A.W. D. Hills and I.C. Wells, in Proc. Int. Conf. on Kinetics of Metallurgical Processes in Steelmaking, Ed. W. Dahl, Verlag Stahleisen, Dusseldorf (1975) pp. 417 - 437.

8. E. Scheil, Z. Metallkunde, 34 (1942) pp. 70 - 72.

9. W.A. Pfann, J. Metals, 4 (1952) pp. 747 - 753.

10. E.T. Turkdogan, Trans. Met. Soc. AIME, 233 (1965) pp. 2100 - 2112.

11. B. Harkness, A. Nicholson and J.D. Murray, J. Iron and Steel Inst., 209 (1971) pp. 692 - 714.

12. A.K. Bagaria and Brahma Deo, Internal Report (1980).

13. A.K. Bagaria, B.Tech. Thesis, Dept. of Met. Engg., I.I.T., Kanpur (1980).

14. A.B. Malage, Internal Report (1979).

15. N.B. Ballal, I.I.T., Bombay; Private Communication.

16. B. Ramadevi and A.B. Malage, Internal Report (1979).

17. E.C. Piggot, Ferrous Analysis Modern Practice and Theory, Chapman and Hall, London (1954).

18. D.R. Kulkarni, B.Tech. Thesis, Dept. of Met. Engg., I.I.T., Kanpur (1982).

19. V.B. Tare, A.V. Ramana Rao and T.A. Ramanarayanam, Solid Electrolytes and Their Application, Ed. E.C. Subba Rao, Plenum Press, New York and London (1980) pp. 165 - 197.

20. B.M. Larsen, T.W. Brower and J.W. Bain, Trans. Met. Soc. AIME, 188 (1950) pp. 854.

21. M. Kenny, J. Metals, 20 (1968) pp. 88.

22. W. Wilson, Trans. Vacuum Met. Conf. Ed. R. Bunshah, Interscience Publishers, New York (1960) pp. 235.

23. M. Kurita, T. Ikeda and K. Marukawa, Trans. I.S.I.J., 11 (1971) pp. 270.

24. N.L. Samways, B.R. Pollard and D.J. Fedenco, Open Hearth Proceedings, 57 (1974) pp. 322.

25. K.P. Abraham, M.W. Davis and F.D. Richardson, Trans. I.S.I., 196 (1960) pp. 82.

26. G.K. Sigworth and J.F. Elliot, Metal Science, 8 (1974) pp. 298.